https://doi.org/10.1093/plcell/koad117 THE PLANT CELL 2023: 35: 2997–3020

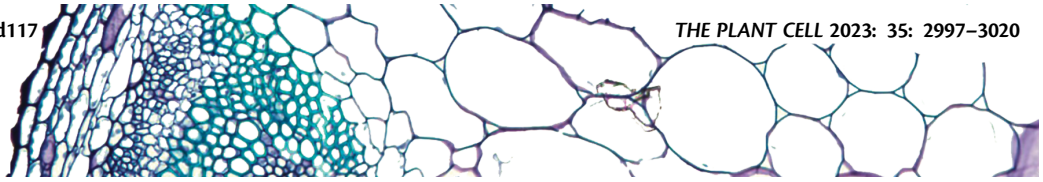

Research Article

Phytochromes enhance SOS2-mediated PIF1 and PIF3 phosphorylation and degradation to promote Arabidopsis salt tolerance

Liang Ma [1,†] Run Han [1,†] Yongqing Yang [1] Xiangning Liu [1] Hong Li [1] Xiaoyun Zhao [1] Jianfang Li [1] Haiqi Fu [1] Yandan Huo [1] Liping Sun [1] Yan Yan [1] Hongyan Zhang [1] Zhen Li [1] Feng Tian [2] Jigang Li [1,*,‡] and Yan Guo [1,*,‡]

1 State Key Laboratory of Plant Environmental Resilience (SKLPER), College of Biological Sciences, China Agricultural University, Beijing 100193, China
2 National Maize Improvement Center, Key Laboratory of Biology and Genetic Improvement of Maize (MOA), Beijing Key Laboratory of Crop Genetic Improvement, China Agricultural University, Beijing 100193, China

*Author for correspondence: guoyan@cau.edu.cn (Y.G.); jigangli@cau.edu.cn (J.L.)
†These authors contributed equally to this work (L.M., R.H.).
‡Senior author.
The authors responsible for the distribution of materials integral to the findings presented in this article in accordance with the policy described in the Instructions for Authors (https://academic.oup.com/plcell/pages/General-Instructions) are Yan Guo (guoyan@cau.edu.cn) and Jigang Li (jigangli@cau.edu.cn).

Abstract

Soil salinity is one of the most detrimental abiotic stresses affecting plant survival, and light is a core environmental signal regulating plant growth and responses to abiotic stress. However, how light modulates the plant's response to salt stress remains largely obscure. Here, we show that Arabidopsis (*Arabidopsis thaliana*) seedlings are more tolerant to salt stress in the light than in the dark, and that the photoreceptors phytochrome A (phyA) and phyB are involved in this tolerance mechanism. We further show that phyA and phyB physically interact with the salt tolerance regulator SALT OVERLY SENSITIVE2 (SOS2) in the cytosol and nucleus, and enhance salt-activated SOS2 kinase activity in the light. Moreover, SOS2 directly interacts with and phosphorylates PHYTOCHROME-INTERACTING FACTORS PIF1 and PIF3 in the nucleus. Accordingly, PIFs act as negative regulators of plant salt tolerance, and SOS2 phosphorylation of PIF1 and PIF3 decreases their stability and relieves their repressive effect on plant salt tolerance in both light and dark conditions. Together, our study demonstrates that photoactivated phyA and phyB promote plant salt tolerance by increasing SOS2-mediated phosphorylation and degradation of PIF1 and PIF3, thus broadening our understanding of how plants adapt to salt stress according to their dynamic light environment.

Introduction

Soil salinity is one of the most detrimental abiotic stresses for plant agriculture. Dramatic progress has been made over the past 30 yr demonstrating that the evolutionarily conserved SALT OVERLY SENSITIVE (SOS) pathway is essential for plant adaptation to salt stress (Zhu 2016; Yang and Guo 2018a, 2018b; Van Zelm et al. 2020; Zhao et al. 2020, Ma et al. 2022). The classical SOS pathway mainly includes 3 types of components: SOS1, a plasma membrane Na^+/H^+ antiporter, SOS2, a serine/threonine protein kinase, and SOS3 and SOS3-LIKE CALCIUM BINDING PROTEIN8 (SCaBP8), 2 calcium-binding proteins (Zhu et al. 1998; Liu et al. 2000; Halfter et al. 2000; Shi et al. 2000; Qiu et al. 2002; Quan et al. 2007). Salt stress induces a rapid increase in cytosolic Ca^{2+} concentrations ($[Ca^{2+}]_{cyt}$) within seconds (Knight et al. 1997; Kiegle et al. 2000; Pan et al. 2012), and the

Received September 19, 2022. Accepted April 10, 2023. Advance access publication April 29, 2023

IN A NUTSHELL

Background: The SALT OVERLY SENSITIVE (SOS) pathway is evolutionarily conserved and essential for plant adaptation to salt stress. The protein kinase SOS2 functions as a network hub in the SOS pathway, and its kinase activity is rapidly activated by salt stress. Activated SOS2 then phosphorylates the Na^+/H^+ antiporter SOS1 at the plasma membrane, thereby activating SOS1 to extrude Na^+ from the cytosol to the apoplast. Phytochromes (phyA and phyB) are the red and far-red light photoreceptors in plants and the PHYTOCHROME-INTERACTING FACTORS (PIFs) are bHLH-family transcription factors that negatively regulate photomorphogenesis. Upon light irradiation, photoactivated phytochromes interact with PIFs in the nucleus and induce their rapid phosphorylation and degradation, thus relieving their repressive effect on photomorphogenesis.

Question: How does the light signal modulate plants' response to salt stress? Does nuclear SOS2 play a role in the salt stress response?

Findings: We show that photoactivated phyA and phyB play important roles in promoting salt stress tolerance, contributing to enhanced salt tolerance of wild-type Arabidopsis seedlings in the light than in the dark. By contrast, PIFs function as the key negative regulators of plant response to salt stress. Moreover, SOS2 directly phosphorylates PIFs, thereby promoting their degradation via the 26S proteasome pathway in response to light. Interestingly, our data indicate that phyA and phyB physically interact with SOS2 and promote its kinase activity under light conditions. Together, our results uncover the molecular mechanism underlying the interplay between light and salt stress pathways that enables plants to acclimate to salt stress under light conditions.

Next steps: We aim to elucidate how photoactivated phyA and phyB promote SOS2 kinase activity. In addition, we will investigate the connections and contributions of cytosolic and nuclear SOS2 in regulating plant salt tolerance.

elevating $[Ca^{2+}]_{cyt}$ is perceived by SOS3 and SCaBP8, which then recruit SOS2 to the plasma membrane and activate its kinase activity (Halfter et al. 2000; Albrecht et al. 2001; Guo et al. 2001; Quintero et al. 2002; Quan et al. 2007). Activated SOS2 then phosphorylates 2 serine residues in the C-terminal auto-inhibitory domain of SOS1, thereby activating SOS1 to extrude Na^+ from the cytosol to the apoplast (Shi et al. 2000, 2002; Qiu et al. 2002; Quintero et al. 2002, 2011).

SOS2 plays an essential role in regulating the SOS pathway, and its kinase activity was shown to be activated by the NaCl treatment within 30 s (Zhu et al. 1998; Halfter et al. 2000; Liu et al. 2000; Lin et al. 2009; Ma et al. 2019). In the absence of salt stress, the SOS pathway is inhibited by several regulators, including ABA INSENSITIVE2 (ABI2; Ohta et al. 2003), GIGANTEA (GI; Kim et al. 2013), 14-3-3 proteins (Zhou et al. 2014), SOS2-LIKE PROTEIN KINASE5 (PKS5; Yang et al. 2019), and BRASSINOSTEROID INSENSITIVE2 (BIN2; Li et al. 2020), all of which interact with SOS2 and repress its kinase activity. In response to salt stress, 14-3-3 proteins and GI are degraded by the ubiquitin/26S proteasome pathway (Kim et al. 2013; Tan et al. 2016). In addition, salt stress also promotes the interactions between 14-3-3 proteins and PKS5, thus relieving PKS5 inhibition of SOS2 kinase activity (Yang et al. 2019). However, although SOS2 was shown to be a nucleocytoplasmic protein (Kim et al. 2007; Quan et al. 2007; Kim et al. 2013), the role of SOS2 in regulating plant salt tolerance is currently understood to occur only on the plasma membrane where SOS2 phosphorylates and activates SOS1, whereas the functional significance of nuclear SOS2 in salt stress response remains completely unknown.

Light not only provides the energy source for photosynthesis, but also serves as an important environmental signal regulating plant development and responses to abiotic stresses. Light signals, including quality, quantity, direction, and duration, are perceived by different families of photoreceptors in plants. In addition to functioning as the red (R) and far-red (FR) light photoreceptors in plants, phytochromes also absorb blue (B) light and play fundamental roles in modulating plant growth and development under various light conditions (Li et al. 2011; Legris et al. 2019; Cheng et al. 2021). The Arabidopsis genome encodes 5 phytochrome photoreceptors, named phytochrome A (phyA) to phyE, and phyA and phyB are the 2 most abundant and important phytochromes in regulating seedling photomorphogenesis (Li et al. 2011; Legris et al. 2019). Phytochromes are localized in the cytosol in dark-grown seedlings; upon light exposure, photoactivated phytochromes translocate into the nucleus where they trigger a signaling cascade that ultimately leads to adaptive changes at the cell and whole organism levels (Fankhauser and Chen 2008; Li et al. 2011; Klose et al. 2015; Legris et al. 2019; Cheng et al. 2021).

PHYTOCHROME-INTERACTING FACTORS (PIFs) are bHLH-family transcription factors that act as negative regulators of photomorphogenesis (Leivar and Quail 2011; Lee and Choi 2017; Pham et al. 2018). There are 8 PIF proteins (PIF1 to PIF8) in Arabidopsis (Lee and Choi 2017), which all contain a conserved motif that mediates their direct interactions with phyB (Khanna et al. 2004; Leivar and Quail 2011). By contrast, only PIF1 and PIF3 possess another conserved motif responsible for interacting with phyA (Leivar and Quail 2011; Oh et al. 2020). The PIF proteins accumulate at

high levels in dark-grown seedlings; upon light irradiation, nuclear-localized phytochromes interact with PIFs and induce their rapid phosphorylation, ubiquitination, and 26S proteasome-mediated degradation (Bauer et al. 2004; Shen et al. 2005; Al-Sady et al. 2006; Nozue et al. 2007; Lorrain et al. 2008; Ni et al. 2013). Several members of protein kinase families, including casein kinase II (CK2; Bu et al. 2011), BIN2 (Bernardo-Garcia et al. 2014; Ling et al. 2017), PHOTO-REGULATORY PROTEIN KINASES (PPKs; Ni et al. 2017), MITOGEN-ACTIVATED PROTEIN KINASE6 (MPK6; Xin et al. 2018), the SUPPRESSOR OF *phyA-105* (SPA) proteins (Paik et al. 2019; Lee et al. 2020), and phytochromes (Shin et al. 2016), have been shown to phosphorylate PIFs and regulate their protein stability. Accumulating evidence has demonstrated that PIFs not only play essential roles in regulating seedling photomorphogenesis, but also act as pivotal integrators of endogenous (e.g. phytohormones and circadian clock) and external (e.g. light and temperature) signaling pathways to optimize plant growth and development (Leivar and Monte 2014; Paik et al 2017).

Emerging evidence has shown that light plays an important role in shaping plant response to salt stress. For instance, it was shown that salinity-induced proline accumulation is memorable, while the light signal is positively involved in salt-induced transcriptional memory of Δ^1-pyrroline-5-carboxylate synthetase 1 (*P5CS1*), encoding the rate-limiting enzyme for proline accumulation (Feng et al. 2016). Another good example is that GI, a repressor of SOS2 activity, acts as a key component in the photoperiodic control of flowering (Mizoguchi et al. 2005; Sawa et al. 2007; Kim et al. 2013). In addition, rice (*Oryza sativa*) PIF-LIKE14 (OsPIL14) and the DELLA protein SLENDER RICE1 (SLR1) form a transcriptional module that integrates light and gibberellin signals to fine-tune seedling growth under salt stress (Mo et al. 2020). Moreover, it was shown that the transcript and protein levels of SOS1 are diurnally regulated in Arabidopsis (Park et al. 2016), suggesting that plant salt stress response may be modulated by the circadian clock. Interestingly, low concentrations of NaCl treatments in soil severely impaired the ability of plants to respond to shade via brassinosteroid and abscisic acid signaling pathways (Hayes et al. 2019). Moreover, PIF4 negatively regulates plant salt tolerance by modulating the expression of many salt stress-responsive genes (Sakuraba et al. 2017). However, although these lines of evidence may suggest a tight connection between the light and salt stress pathways, compelling evidence supporting the direct associations between the key components of the 2 pathways is still lacking.

In this study, we show that PIFs function as the key negative regulators of plant response to salt stress. Moreover, SOS2 directly phosphorylates PIFs, thereby promoting their degradation via the 26S proteasome pathway in response to light. Interestingly, our data indicate that phyA and phyB physically interact with SOS2 and promote its kinase activity under light conditions. Together, our study uncovers the molecular mechanism underlying the interplay between light and salt stress pathways that enables plants to better adapt to salt stress under light conditions.

Results

Phytochromes promote plant salt stress tolerance in the light

To investigate how light modulates plant tolerance to salt stress, we first compared the germination rates of wild-type (WT) (Col) seeds grown on half-strength (1/2) MS medium under continuous white (W) light or dark (D) conditions with or without 125 mM NaCl. As shown in Fig. 1, A and B, whereas no obvious difference in germination rates was observed for Col seeds grown under light and dark conditions in the absence of NaCl, the exogenous addition of 125 mM NaCl caused a stronger inhibition of germination for Col seeds growing in the dark than in the light. Moreover, when we grew Col seedlings vertically on 1/2 MS medium in the light or darkness for various days in the presence and absence of 125 mM NaCl, we observed that the seedlings were well established (i.e. complete emergence of hypocotyls and cotyledons) after growing for 7 d in both light and dark conditions in the absence of NaCl; however, in the presence of 125 mM NaCl, the establishment rates were remarkably higher (~50% to 65% relative to the dark treatment) for seedlings grown in the light than those grown in the dark (Fig. 1, C and D). Collectively, our data demonstrate that Arabidopsis seedlings are more tolerant to salt stress in the light than in the dark.

To examine whether light may regulate the accumulation of Na^+ in Arabidopsis seedlings, we first grew Col seedlings vertically on 1/2 MS medium without NaCl in the light for 7 d, and then moved them to 1/2 MS medium containing 0 or 100 mM NaCl, respectively, and allowed them to grow in light or dark conditions for another 6 d. Next, we measured the Na^+ contents in these seedlings and our results showed that there was no significant difference in the Na^+ contents for seedlings grown under light and dark conditions in the absence of NaCl treatment (Fig. 1E). However, when Col seedlings were treated with 100 mM NaCl, we observed an enhanced accumulation of Na^+ in both shoots and roots, and interestingly, the Na^+ contents in shoots and roots of Col seedling grown in the dark were both higher than those grown in the light (Fig. 1E). These results suggest that light may promote plant salt tolerance by reducing the Na^+ contents.

Because of the fundamental roles of phytochromes in modulating plant growth and development under various light conditions (Li et al. 2011; Legris et al. 2019; Cheng et al. 2021), we asked whether phytochromes are responsible for the light-enhanced tolerance of Arabidopsis seedlings to salt stress. To this end, we first examined the contribution of the 2 most important phytochromes, phyA and phyB, to salt tolerance. We first grew Col and *phyA-211* mutant seedlings vertically on 1/2 MS medium without NaCl for 7 d, and then

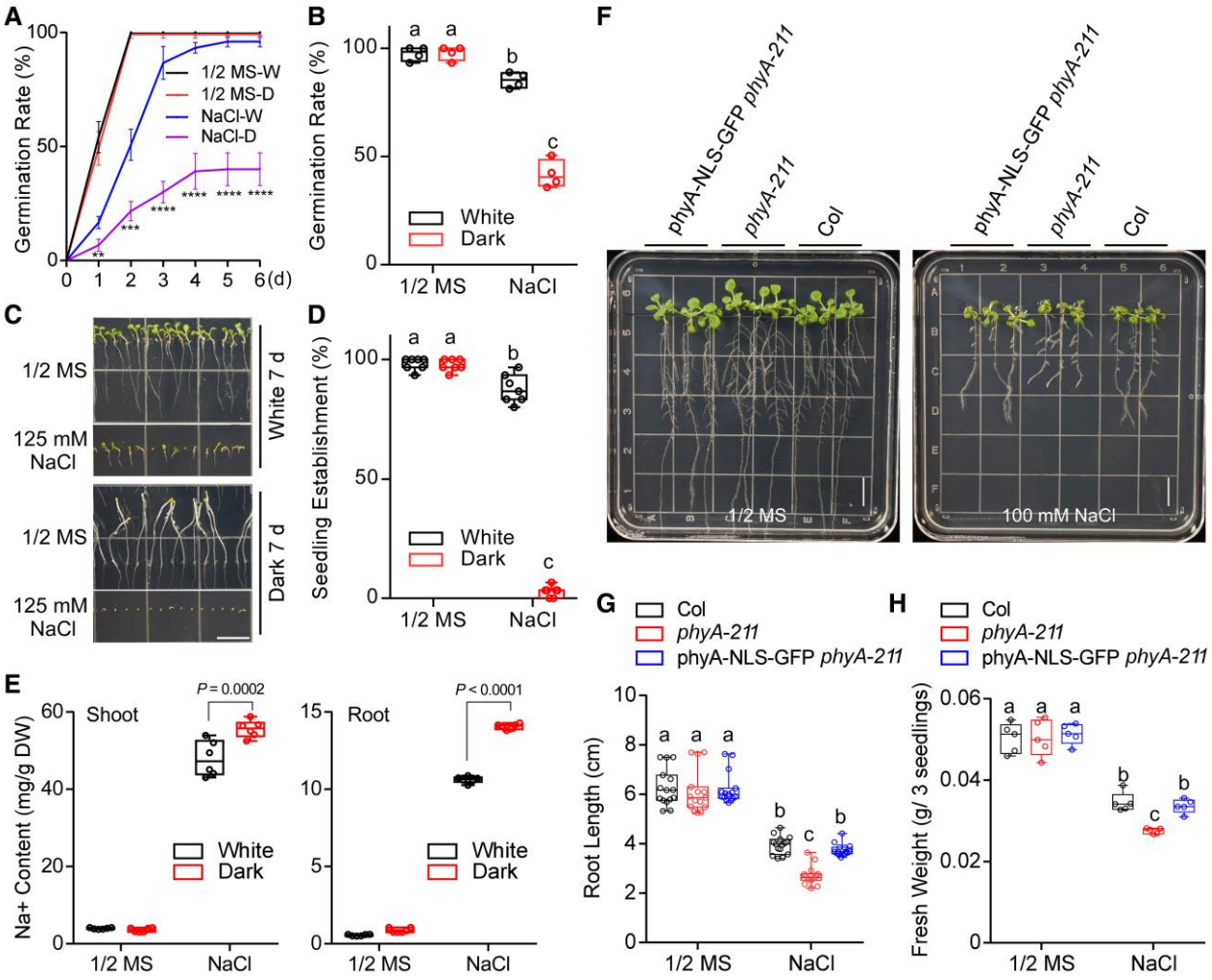

Figure 1. Phytochromes promote plant salt stress tolerance in the light. **A)** Germination rate measurement. Imbibed seeds of WT (Col) were sown on 1/2 MS medium containing 0 or 125 mM NaCl, grown in white light (W) or dark (D) conditions, and then seed germination rates were calculated at the indicated times. Germination was defined as the first sign of radicle tip emergence and scored daily until the 6th day of incubation. Data are the means ± SE ($n = 4$, each pool containing at least 45 seeds). $^{**}P < 0.01$, $^{***}P < 0.001$, $^{****}P < 0.0001$ (Student's *t*-test; **Supplemental Data Set 2**) for the comparations for Col treated with 125 mm NaCl between light and dark conditions. **B)** Germination rate measurement. Imbibed WT (Col) seeds were sown on 1/2 MS medium containing 0 or 125 mM NaCl, grown in light or dark conditions for 7 d, and then seed germination rates were calculated. Germination was defined as the first sign of radicle tip emergence ($n = 4$, each pool containing at least 45 seeds). Different letters represent significant differences determined by two-way ANOVA with Tukey's post hoc test ($P < 0.05$; **Supplemental Data Set 2**). **C)** Arabidopsis seedlings displayed enhanced salt tolerance in the light than in the dark. WT (Col) seedlings were grown vertically on 1/2 MS medium containing 0 or 125 mM NaCl in light or dark conditions for indicated times. Scale bar = 1 cm. **D)** Seedling establishment rate measurements. Col seedlings were grown on 1/2 MS medium containing 0 or 125 mM NaCl in light and dark conditions for 7 d. ($n = 7$, each pool containing 40 seedlings). Different letters represent significant differences determined by two-way ANOVA with Tukey's post hoc test ($P < 0.05$; **Supplemental Data Set 2**). The rates of seedling establishment were measured based on the criteria recently used by previous studies (Yadukrishnan et al. 2020; Peng et al. 2022) that hypocotyls and cotyledons should emerge completely in established seedlings. **E)** The shoot and root Na^+ contents of plants grown under control and 100 mM NaCl in the light or in the dark. The seedlings were first grown vertically on 1/2 MS without NaCl in continuous white light for 7 d, then transferred to 1/2 MS medium containing 0 or 100 mM NaCl and grown in light or dark conditions for additional 6 d, and then the shoots and roots were harvested separately. A pool containing more than 60 individual plants represented 1 biological replicate ($n = 6$), *P*-value was determined by Student's *t*-test (**Supplemental Data Set 2**). **F–H)** Phenotypes **(F)**, root lengths **(G)**, and fresh weights **(H)** of Col, *phyA-211*, and *ProPHYA:phyA-NLS-GFP phyA-211* seedlings grown on 0 or 100 mM NaCl in white light. The seedlings were first grown vertically on 1/2 MS medium without NaCl in continuous white light for 7 d, and then transferred to 1/2 MS medium containing 0 or 100 mM NaCl and grown in continuous white light for additional 6 d. In **(F)**, scale bar = 1 cm. In **(G)**, $n = 15$, and in **(H)**, $n = 5$ (5 plates from 5 independent assays, with 3 seedlings on each plate weighed together). Different letters represent significant differences determined by two-way ANOVA with Tukey's post hoc test ($P < 0.05$; **Supplemental Data Set 2**).

moved them to 1/2 MS medium containing 0 or 100 mM NaCl, respectively, and allowed them to grow in the light for another 6 d. Interestingly, whereas no significant differences in root lengths and fresh weights were observed for Col and *phyA-211* mutant seedlings growing on 1/2 MS medium without NaCl, salt treatment caused a stronger inhibition of primary root and seedling growth in *phyA-211* mutants than in Col seedlings (Fig. 1, F to H). Similarly, we also observed that *phyB-9* and *phyA-211 phyB-9* mutants displayed salt-sensitive phenotypes compared with Col seedlings (Supplemental Fig. S1).

It was previously shown that the introduction of the constitutively nuclear-localized phyA-NLS-GFP under the control of the native *PHYA* promoter could fully rescue the FR-insensitive phenotypes of *phyA-211* mutants (Genoud et al. 2008). Notably, phyA-NLS-GFP successfully rescued the salt-sensitive phenotypes of *phyA-211* mutants (Fig. 1, F to H), indicating that the decreased salt tolerance of *phyA-211* mutants was indeed caused by the loss of phyA function. Moreover, *phyA-211* mutant seedlings displayed salt-sensitive phenotypes on 1/2 MS medium with or without sucrose (Fig. 1, F to H; Supplemental Fig. S2, A to C), indicating that the role of phyA in regulating salt tolerance is not affected by sucrose. In addition, *phyA-211* mutant seedlings did not exhibit any differences compared with Col when grown on 1/2 MS medium containing 250 mM mannitol, indicating that the salt-sensitive phenotype of *phyA-211* mutant seedlings was not due to the osmotic stress caused by salt stress (Supplemental Fig. S2, D to F). Together, both phyA and phyB play important roles in promoting salt stress tolerance in the light.

To further substantiate the role of phyA in regulating salt tolerance in saline soil, we transferred 10-d-old light-grown Col, *phyA-211*, and *ProPHYA:phyA-NLS-GFP phyA-211* seedlings to soil and allowed them to grow for an additional 2 wk, followed by treatment with or without 200 mM NaCl for 1.5 to 2.0 wk. Consistently, we observed that whereas NaCl treatment inhibited the seedling growth of all genotypes, the degree of inhibition was greater in *phyA-211* than in Col and *ProPHYA:phyA-NLS-GFP phyA-211* seedlings (Supplemental Fig. S3), thus reinforcing the notion that phyA positively regulates plant salt tolerance.

To investigate whether phyA enhances plant salt tolerance by reducing the accumulation of Na^+ in the seedlings, we measured the Na^+ contents in Col, *phyA-211*, and *ProPHYA:phyA-NLS-GFP phyA-211* seedlings treated with mock (1/2 MS) or 100 mM NaCl. Interestingly, whereas no significant differences in Na^+ contents were observed in Col and *phyA-211* mutant seedlings grown on 1/2 MS medium without NaCl, salt treatment led to a higher accumulation of Na^+ in both roots and shoots of *phyA-211* mutant than in Col seedlings. The fact that phyA-NLS-GFP successfully rescued the overaccumulation of Na^+ in *phyA-211* mutant seedlings (Supplemental Fig. S4) indicated that phyA indeed decreases the Na^+ accumulation under salt stress. Taken together, our data demonstrate that the phytochrome photoreceptors positively regulate plant salt tolerance in the light by reducing the toxic effect caused by salt stress.

PhyA and phyB promote SOS2 kinase activity in the light

Considering the pivotal role of SOS2 in the SOS pathway and plant salt tolerance (Zhu et al. 1998; Halfter et al. 2000; Liu et al. 2000; Cheng et al. 2004; Ma et al. 2022), we next asked whether SOS2 may be involved in enhanced salt tolerance in the light. To this end, we first obtained a T-DNA insertion mutant for *SOS2*, named *sos2-T1* (SALK_016683), in which the T-DNA was inserted into the 11th intron of *SOS2* (Supplemental Fig. S5). We then compared the rates of seed germination and seedling establishment of Col and *sos2-T1* mutants grown in darkness or continuous light conditions. Our results showed that without salt stress, there was no obvious difference in the rates of seed germination and seedling establishment between Col and *sos2-T1* mutant grown in both light and dark conditions (Fig. 2, A to C). However, the *sos2-T1* mutant exhibited lower seed germination and seedling establishment rates than Col under salt stress in both light and dark conditions (Fig. 2, A to C). Notably, the role of SOS2 in promoting seedling growth under salt stress was more prominent in the light than in the dark (Fig. 2C). Together, our results indicated that SOS2 plays a predominant role in regulating salt tolerance in both light and dark conditions, with a more prominent role in the light.

Next, we asked whether the kinase activity of SOS2 could be regulated by light. We grew *Pro35S:Myc-SOS2* seedlings in darkness or continuous FR, R, B, and W light conditions for 4 d, and then treated them with mock or 100 mM NaCl for 12 h. Subsequently, Myc-SOS2 proteins were purified by immunoprecipitation with anti-Myc Affinity Gel and subjected to semi-in vivo kinase assays by incubation with His-SCaBP8, a specific substrate of SOS2 (Lin et al. 2009). As shown in Fig. 2, D and E, SCaBP8 was remarkably phosphorylated by SOS2 in response to NaCl treatment, consistent with our previous reports (Lin et al. 2009; Ma et al. 2019). Strikingly, we observed that salt and light stimuli synergistically increase SOS2 kinase activity (Fig. 2, D and E). These data thus may explain why SOS2 plays a more prominent role in promoting plant salt tolerance in the light. In addition, the fact that SOS2 displayed the highest kinase activity in R light among all light conditions (Fig. 2, D and E) suggested that R light-activated phytochromes may be involved in promoting SOS2 kinase activity.

To investigate the role of phyA and phyB in promoting SOS2 kinase activity in the light, we generated homozygous *Pro35S:Myc-SOS2 phyA phyB* transgenic seedlings, grew them together with *Pro35S:Myc-SOS2* under continuous W light for 4 d, and performed semi-in vivo kinase assays using immunoprecipitated Myc-SOS2 and recombinant His-SCaBP8 proteins. Our data indicated that salt-induced SOS2 kinase activity in the light was greatly impaired in the absence of phyA and phyB (Fig. 2, F and G), demonstrating

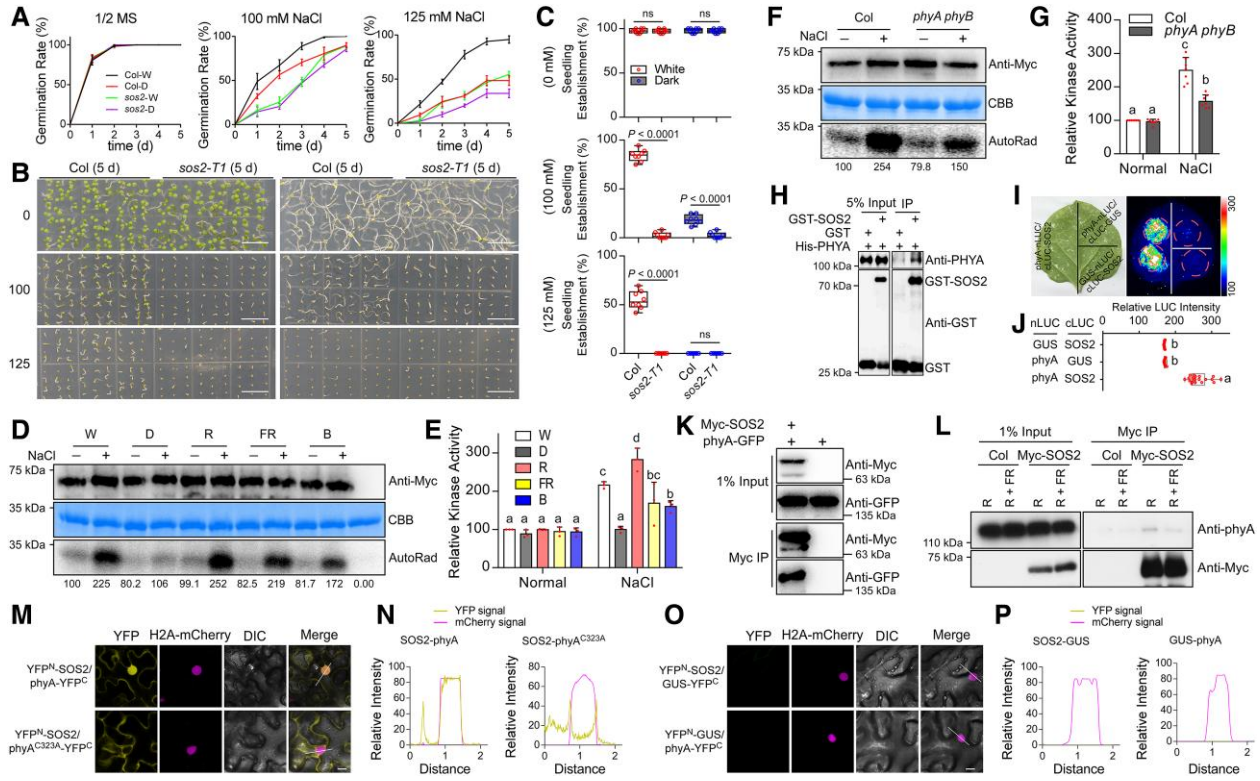

Figure 2. PhyA and phyB physically interact with SOS2 to promote SOS2 kinase activity in the light. **A)** Germination rate measurement. Imbibed seeds of the WT (Col) or *sos2-T1* mutants were sown on 1/2 MS medium containing 0, 100, or 125 mM NaCl, grown in light or dark conditions, and then seed germination rates were calculated at the indicated times. Germination was defined as the first sign of radicle tip emergence and scored daily until the 6th day of incubation. Data are the means ± SD ($n = 4$). **B)** Growth of Col and *sos2-T1* seedlings grown on different concentrations of NaCl in white light or dark conditions. Col and *sos2-T1* seeds were sown on 1/2 MS medium containing 0, 100, or 125 mM NaCl and grown in continuous white light or dark conditions for 5 d. Scale bar = 1 cm. **C)** Seedling establishment rate measurements. Col and *sos2-T1* seedlings were grown on 1/2 MS medium containing 0, 100, or 125 mM NaCl in light and dark conditions for 5 d; ($n = 8$), each pool containing 40 seedlings. Significant differences were determined by two-way ANOVA with Tukey's post hoc test (**Supplemental Data Set 2**). ns, not significant. **D)** Salt-induced SOS2 kinase activity more predominantly in the light than in the dark. *Pro35S:Myc-SOS2* seedlings were grown in darkness or continuous FR, R, B, and W light conditions for 4 d, and then treated with mock or 100 mM NaCl for 12 h. The top panel shows the immunoprecipitated Myc-SOS2 proteins by immunoblotting, the middle panel shows Coomassie Brilliant Blue (CBB)-stained SDS-PAGE gel containing His-SCaBP8 proteins, and the bottom panel shows autoradiograph indicating SOS2 kinase activity. Numbers below the autoradiograph indicate the relative band intensities of SOS2 kinase activity normalized to those of the immunoprecipitated Myc-SOS2 proteins, respectively. The ratio of the first band was set to 100 for the gel. **E)** Statistical analysis of the relative kinase activity values shown in **(D)**. Error bars indicated the means ± SD ($n = 3$). Different letters represent significant differences determined by two-way ANOVA with Tukey's post hoc test ($P < 0.05$; **Supplemental Data Set 2**). **F)** PhyA and phyB enhance salt-induced SOS2 kinase activity in the light. *Pro35S:Myc-SOS2* and *Pro35S:Myc-SOS2 phyA phyB* seedlings were grown in continuous W light for 4 d, and then treated with mock or 100 mM NaCl for 12 h. The top panel shows the immunoprecipitated Myc-SOS2 proteins by immunoblotting, the middle panel shows CBB-stained SDS-PAGE gel containing His-SCaBP8 proteins, and the bottom panel shows autoradiograph indicating SOS2 kinase activity. Numbers below the autoradiograph indicate the relative band intensities of SOS2 kinase activity normalized to those of the immunoprecipitated Myc-SOS2 proteins, respectively. The ratio of the first band was set to 100 for the gel. **G)** Statistical analysis of the relative kinase activity values shown in **(F)**. Error bars indicated the means ± SD ($n = 7$). Different letters represent significant differences determined by two-way ANOVA with Tukey's post hoc test ($P < 0.05$; **Supplemental Data Set 2**). **H)** Pull-down assays show that GST-tagged SOS2, but not GST alone, was able to pull down His-PHYA in vitro. Input, 5% of the purified His-tagged target proteins were loaded. **I)** LCI assays show the interactions between phyA and SOS2 in plant cells. The indicated combinations of constructs were transfected into *N. benthamiana* leaves, respectively, and the LUC activity was detected 3 d after infiltration. The infiltration areas were circled with red dotted lines. The color gradient scale represents the relative intensities of the luciferase signal provided by the cold CCD camera (Nikon-L936; Andor Tech). **J)** Statistical analysis of the relative fluorescence intensity values shown in **(I)**. At least 3 independent assays were performed, with 8 *N. benthamiana* leaves for each assay. $n = 20$, different letters represent significant differences determined by one-way ANOVA with Tukey's post hoc test ($P < 0.05$; **Supplemental Data Set 2**). **K)** Co-IP assays show that SOS2 interacts with phyA in vivo. Myc-SOS2 and phyA-GFP fusion proteins were transiently expressed in Arabidopsis leaf protoplasts. The total proteins were extracted and incubated with anti-Myc Affinity Gel (Sigma-Aldrich). The total (1% input) and precipitated proteins were examined by immunoblotting using anti-Myc and anti-GFP antibodies, respectively. **L)** Co-IP assays show that SOS2 exhibits a higher affinity to active phyA in vivo. Four-day-old etiolated Col and *Pro35S:Myc-SOS2* were extracted and treated with 5 min of R light (active phyA) or with 5 min of R light plus 5 min of FR light (inactive phyA) and then incubated with anti-Myc Affinity Gel (Sigma-Aldrich). The total (1% input) and precipitated proteins

(continued)

that phyA and phyB indeed enhance salt-induced SOS2 kinase activity in the light.

PhyA and phyB physically interact with SOS2

Next, we asked whether phyA and phyB could physically interact with SOS2 to directly regulate its kinase activity. To this end, we first performed in vitro pull-down assays by using GST-tagged SOS2 (GST-SOS2) and His-tagged PHYA (His-PHYA) purified from *Escherichia coli*. Our pull-down assays showed that GST-tagged SOS2, but not GST alone, was able to pull down His-tagged PHYA in vitro (Fig. 2H). To substantiate the interaction between SOS2 and phyA *in planta*, we performed firefly luciferase (LUC) complementation imaging (LCI) assays by transiently co-expressing phyA-nLUC and cLUC-SOS2 proteins in *Nicotiana benthamiana* leaves. As shown in Fig. 2, I and J, co-expression of phyA-nLUC and cLUC-SOS2 led to strong LUC activity, whereas phyA-nLUC or cLUC-SOS2 co-transformed with control constructs showed only background levels of LUC activity. To further verify the interaction between phyA and SOS2 in vivo, *phyA-GFP* and *Myc-SOS2* were transiently co-expressed in Arabidopsis leaf protoplasts, and then coimmunoprecipitation (co-IP) assays were performed using anti-Myc Affinity Gel. Our immunoblot data showed that phyA-GFP was coprecipitated by anti-Myc antibodies in the presence of Myc-SOS2 (Fig. 2K), indicating that SOS2 was associated with phyA in vivo. Together, these data indicate that SOS2 physically interacts with phyA.

Since phytochromes exist in vivo in 2 interconvertible forms, i.e. R light-absorbing Pr form (biologically inactive) and FR light-absorbing Pfr form (biologically active) (Bae and Choi 2008; Li et al. 2011; Legris et al. 2019; Cheng et al. 2021), we asked which form of phyA associated with SOS2 more strongly. To this end, we conducted co-IP assays using Col and *Pro35S:Myc-SOS2* seedlings grown in the dark for 4 d. The total proteins were extracted in the dark and exposed to R light for 5 min (converting phytochromes to Pfr form), or R light for 5 min plus FR light for 5 min (converting phytochromes back to Pr form). Our results showed that more phyA-Pfr coprecipitated with Myc-SOS2 after R light treatment than R plus FR light treatment (Fig. 2L), indicating that SOS2 interacted preferentially with the Pfr form of phyA in vivo.

It was previously shown that light exposure induces rapid import of phytochromes into the nucleus, whereas nuclear-localized phytochromes initiate light signaling by interacting with numerous signal transducers (Bae and Choi 2008; Fankhauser and Chen 2008; Li et al. 2011; Klose et al. 2015; Li and Hiltbrunner 2021). To investigate whether phyA interacts with SOS2 in the nucleus in the light, we performed bimolecular fluorescence complementation (BiFC) assays by co-expressing YFP^N-SOS2 (full-length SOS2 protein fused with the N-terminal domain of YFP) and phyA-YFP^C (full-length phyA fused with the C-terminal domain of YFP) proteins in *N. benthamiana* leaves. We observed that phyA and SOS2 could interact in the nucleus, as indicated by H2A-mCherry, a nuclear localization marker (Fig. 2, M to P). By contrast, SOS2 interacts with $phyA^{C323A}$, an inactive phyA variant, in the cytosol but not in the nucleus (Fig. 2, M and N), consistent with previous report that $phyA^{C323A}$ is constitutively localized in the cytosol (Rausenberger et al. 2011).

We also examined whether SOS2 could interact with phyB. Our in vitro pull-down LCI, BiFC, and co-IP assay results showed that SOS2 could also physically interact with phyB in both the nucleus and the cytosol, with a stronger affinity with phyB-Pfr than phyB-Pr (Supplemental Fig. S6). Collectively, our data demonstrate that SOS2 physically interacts with both phyA and phyB.

PhyA regulates plant salt tolerance in the light by promoting SOS2 kinase activity

To determine the genetic relationships between *SOS2* and *phyA*, we generated *phyA-211 sos2-T1* double mutants by genetic crossing. We first grew Col, *phyA-211*, *sos2-T1*, and *phyA-211 sos2-T1* mutant seedlings vertically in the light without NaCl for 7 d, and then transferred them to 1/2 MS medium containing 0, 35, or 100 mM NaCl, respectively, and allowed them to grow vertically in the light for another 5 d. Whereas no significant difference in seedling growth was observed for all tested genotypes in the absence of NaCl, *phyA-211 sos2-T1* mutants displayed an extremely salt-sensitive phenotype, similar to *sos2-T1* mutants, under all tested concentrations of NaCl treatments (Fig. 3, A to C). Together, we conclude that *SOS2* is epistatic to *phyA* in mediating plant salt tolerance.

Next, we asked whether phyA regulates plant salt tolerance in the light through SOS2. R and FR light are the spectra that phyA and phyB exhibit maximal activity, respectively (Li and Hiltbrunner 2021). Notably, salt-induced SOS2 kinase activity in the light was greatly impaired in the absence of phyA and phyB (Fig. 2, F and G); however, the levels of endogenous SOS2 proteins were not obviously decreased in both FR-grown *phyA* and R-grown *phyB* mutants (Supplemental Fig. S7). Thus, we reasoned that the salt-sensitive phenotype of *phyA-211* mutants may result from reduced SOS2 kinase activity rather than reduced SOS2 protein abundance in the absence of phyA. To test this hypothesis, we generated

Figure 2. (Continued)
were examined by immunoblotting using anti-Myc and anti-phyA antibodies, respectively. **M and O)** BiFC assays show that SOS2 interacts with phyA in the nucleus of *N. benthamiana* leaf cells. H2A-mCherry, the nuclear localization marker. An unrelated protein (GUS) was used as the negative control. Scale bar = 20 μm. **N and P)** The fluorescence intensities (YFP and mCherry signals) over the white lines shown in **(M)** and **(O)** were scanned using the ImageJ plot profile tool. The *y*-axes indicate relative pixel intensity. Distance indicates the relative positions on the white lines.

transgenic Arabidopsis plants, in either *sos2-T1* or *phyA-211* mutant background, to express WT SOS2 or the constitutively active SOS2^{T168D} mutant (phosphorylation mimicry of Thr-168 in the activation-loop of SOS2 resulting in a superactive form of SOS2; Guo et al. 2001) under the control of the *UBQ10* promoter. Since our data indicated that SOS2 interacts with phyA in the nucleus in the light (Fig. 2M), a nuclear localization signal (NLS) was added upstream of YFP-tagged SOS2 to facilitate its nuclear translocation. Our observations made from confocal microscopy indicated that indeed, both NLS-YFP-SOS2 and NLS-YFP-SOS2^{T168D} are constitutively localized in the nucleus in both *phyA-211* and *sos2-T1* mutant backgrounds (Fig. 3D; Supplemental Fig. S8, A and B). Interestingly, we observed that both NLS-YFP-SOS2 and NLS-YFP-SOS2^{T168D} appeared to fully rescue the salt-sensitive phenotype of *sos2* mutants (Supplemental Fig. S8, C to H), indicating that the nuclear-localized SOS2 is important for plant salt tolerance. Moreover, our data further showed that NLS-YFP-SOS2^{T168D} partially rescued the salt-sensitive phenotype of *phyA-211* mutant seedlings grown in the light (Fig. 3, E to G). However, the nuclear-localized WT SOS2 failed to rescue the primary root growth and fresh weight phenotypes of *phyA-211* mutant seedlings grown under salt stress (Supplemental Fig. S9). Collectively, our data suggest that phyA regulates plant salt tolerance in the light by promoting salt-induced SOS2 kinase activity.

PIFs contribute to the salt-sensitive phenotype of *sos2* mutants

Next, we investigated how SOS2 mediates plant salt stress tolerance in the nucleus. Accumulating evidence indicates that PIFs act as a molecular hub mediating light control of plant abiotic stress response (Jiang et al. 2017; Han et al. 2019; Zhou et al. 2019; Dong et al. 2020, Qi et al. 2020); therefore, we asked whether PIFs are involved in SOS2-regulated salt stress pathway in the nucleus. We first compared the germination rates of *pifq* (*pif1 pif3 pif4 pif5*) mutant seeds with those of Col sown on 1/2 MS medium containing 0 or 125 mM NaCl. Our results showed that *pifq* displayed greater resistance to salt-inhibited seed germination in both light and dark conditions (Fig. 4A; Supplemental Fig. S10A). In addition, in the presence of 125 mM NaCl, the seedling establishment rates of both dark- and light-grown *pifq* mutants were much higher than those of Col (Fig. 4, B and C; Supplemental Fig. S10, B and C), indicating *pifq* mutant seedlings were more resistant to NaCl treatment than Col. Further analyses of the individual *PIF* mutant and overexpression lines revealed that *pif1*, *pif3*, and *pif4* single mutant seedlings displayed increased tolerance to salt stress in darkness (Supplemental Fig. S10D). Together, these data demonstrate that PIFs play a negative role in regulating salt stress tolerance in Arabidopsis.

To further substantiate the role of PIFs in regulating salt tolerance in saline soil, we further transferred 10-d-old light-grown Col and *pifq* mutant seedlings to soil and allowed them to grow for an additional 2 wk, followed by treatment with 150 mM NaCl for 1.5 to 2.0 wk. The *pifq* mutants were more tolerant than Col to salt treatment (Supplemental Fig. S11, A to C), thus reinforcing the notion that PIFs negatively regulate plant salt tolerance.

To further investigate the genetic interaction between *PIFs* and *SOS2*, we generated the *sos2-T1 pifq* pentuple mutants by genetic crossing, and compared their germination rates with Col, *sos2-T1*, and *pifq* seeds in response to salt stress. Our data showed that the germination rates of *sos2-T1 pifq* were similar to those of Col, *sos2-T1*, and *pifq* seeds in both light and dark conditions without salt stress; however, under the treatment of 125 mM NaCl, mutation of 4 *PIF* genes could partially rescue the salt-inhibited germination of *sos2-T1* seeds in both light and dark conditions (Fig. 4D; Supplemental Fig. S11D). In addition, mutations of 4 *PIF* genes could also partially rescue the salt-hypersensitive phenotypes of *sos2-T1* seedlings in the light under 100 mM NaCl treatment (Supplemental Fig. S11, E and F). Notably, the soil-grown *sos2-T1 pifq* pentuple seedlings displayed a decreased sensitivity to NaCl treatment than that of *sos2-T1* mutants (Supplemental Fig. S11, A to C), indicating that PIFs might function in the same pathway as SOS2 to mediate salt stress response in Arabidopsis.

To verify this conclusion, we then grew Col, *pifq*, *sos2-T1*, and *sos2-T1 pifq* pentuple mutant seedlings in the light without NaCl for 7 d, then transferred them to 1/2 MS medium containing 0 or 35 mM NaCl, and then allowed them to grow in the light for another 5 d. Whereas no significant difference in primary root growth was observed for all tested seedlings in the absence of NaCl, *sos2-T1 pifq* pentuple mutant seedlings displayed an intermediate primary root growth, between that of the Col and *sos2-T1* mutant seedlings under NaCl treatment (Fig. 4, E and F). Similarly, we also observed that mutation of 4 *PIF* genes led to an obviously decreased Na^+ contents in both roots and shoots of not only Col, but also *sos2-T1* mutant seedlings under NaCl treatment (Supplemental Fig. S12). These data indicated that PIFs contribute to the salt-sensitive phenotype of *sos2-T1* mutants.

SOS2 mediates salt-induced degradation of PIF proteins

Next, we asked how PIFs are regulated by salt stress. Since both phyA and phyB play important roles in conferring enhanced salt stress tolerance in the light (Fig. 1; Supplemental Fig. S1), we examined the regulatory effect of salt stress on protein stability of PIF1 and PIF3, 2 PIF proteins that interact with both phyA and phyB (Leivar and Quail 2011; Pham et al. 2018). We grew homozygous *Pro35S:PIF1-Myc* and *Pro35S:PIF3-Myc* seedlings in darkness for 4 d, and then treated them with cycloheximide (CHX), a protein synthesis inhibitor, or CHX plus 100 mM NaCl treatments. Our immunoblot data showed

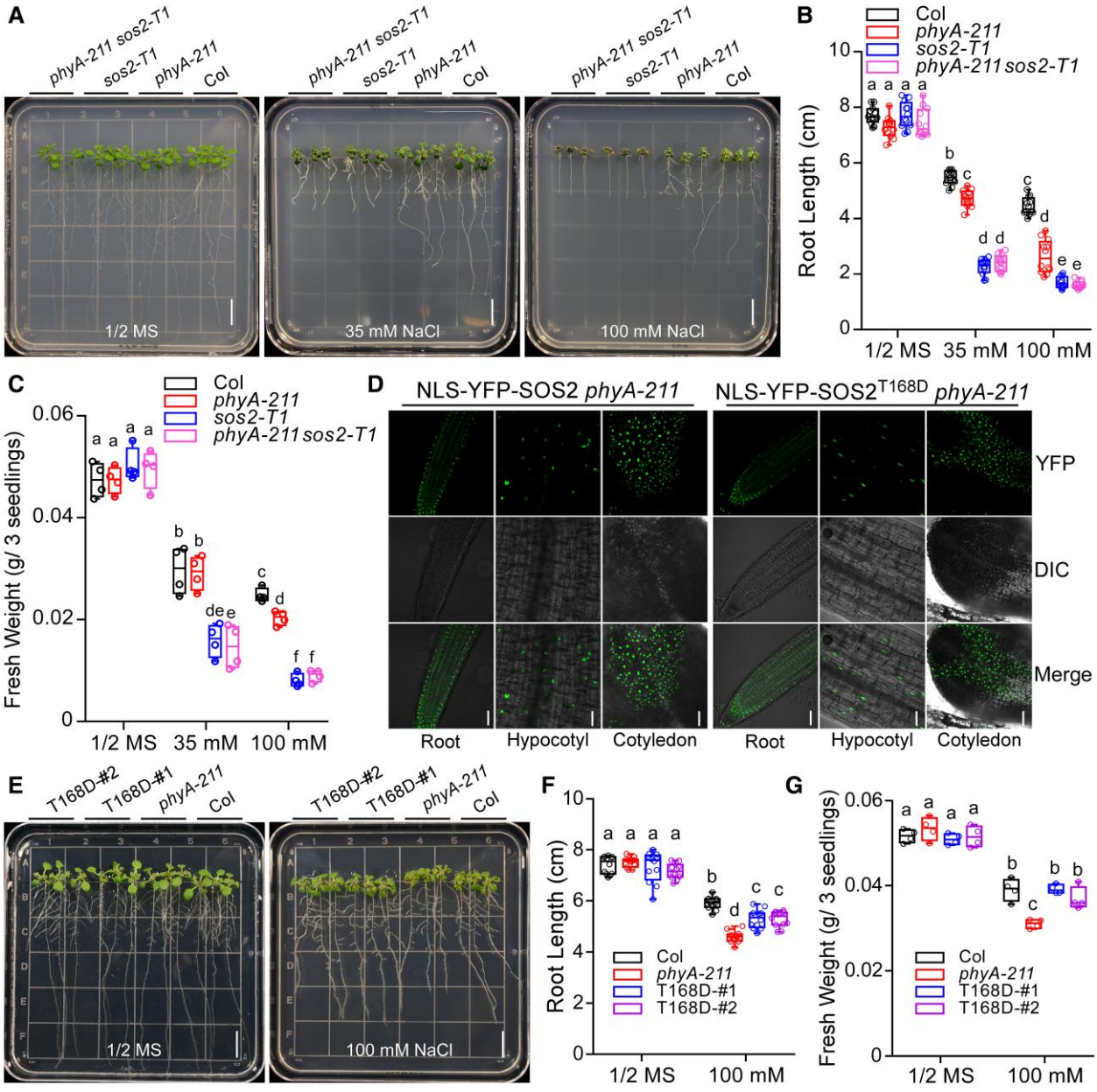

Figure 3. PhyA regulates plant salt tolerance in the light by promoting SOS2 kinase activity. **A–C)** Phenotypes **(A)**, root lengths **(B)**, and fresh weights **(C)** of WT (Col), *phyA-211*, *sos2-T1*, and *phyA sos2-T1* mutant seedlings grown on different concentrations of NaCl in white light. The seedlings were first grown vertically on 1/2 MS medium without NaCl in continuous white light for 7 d, and then transferred to 1/2 MS medium containing 0, 35, or 100 mM NaCl and grown in continuous white light for additional 5 d. In **(A)**, scale bar = 1 cm. In **(B)**, $n = 12$, and in **(C)**, $n = 4$ (4 plates from 4 independent assays, with 3 seedlings on each plate weighed together). Different letters represent significant differences determined by two-way ANOVA with Tukey's post hoc test ($P < 0.05$; **Supplemental Data Set 2**). **D)** Nuclear localization of NLS-YFP-SOS2 and NLS-YFP-SOS2^{T168D} in the root, hypocotyl, and cotyledon cells of *phyA-211* mutant seedlings. The seedlings were grown in continuous white light for 4 d and then examined using fluorescence microscopy. Scale bar = 10 μm. **E–G)** Phenotypes **(E)**, root lengths **(F)**, and fresh weights **(G)** of Col, *phyA-211*, and 2 homozygous *ProUBQ10:NLS-YFP-SOS2^{T168D}* *phyA-211* lines grown on different concentrations of NaCl in white light. The seedlings were first grown vertically on 1/2 MS medium without NaCl in continuous white light for 7 d, and then transferred to 1/2 MS medium containing 0 or 100 mM NaCl and grown under continuous white light for additional 7 d. In **(E)**, scale bar = 1 cm, in **(F)**, $n = 12$, and in **(G)**, $n = 4$ (4 plates from 4 independent assays, with 3 seedlings on each plate weighed together). Different letters represent significant differences determined by two-way ANOVA with Tukey's post hoc test ($P < 0.05$; **Supplemental Data Set 2**).

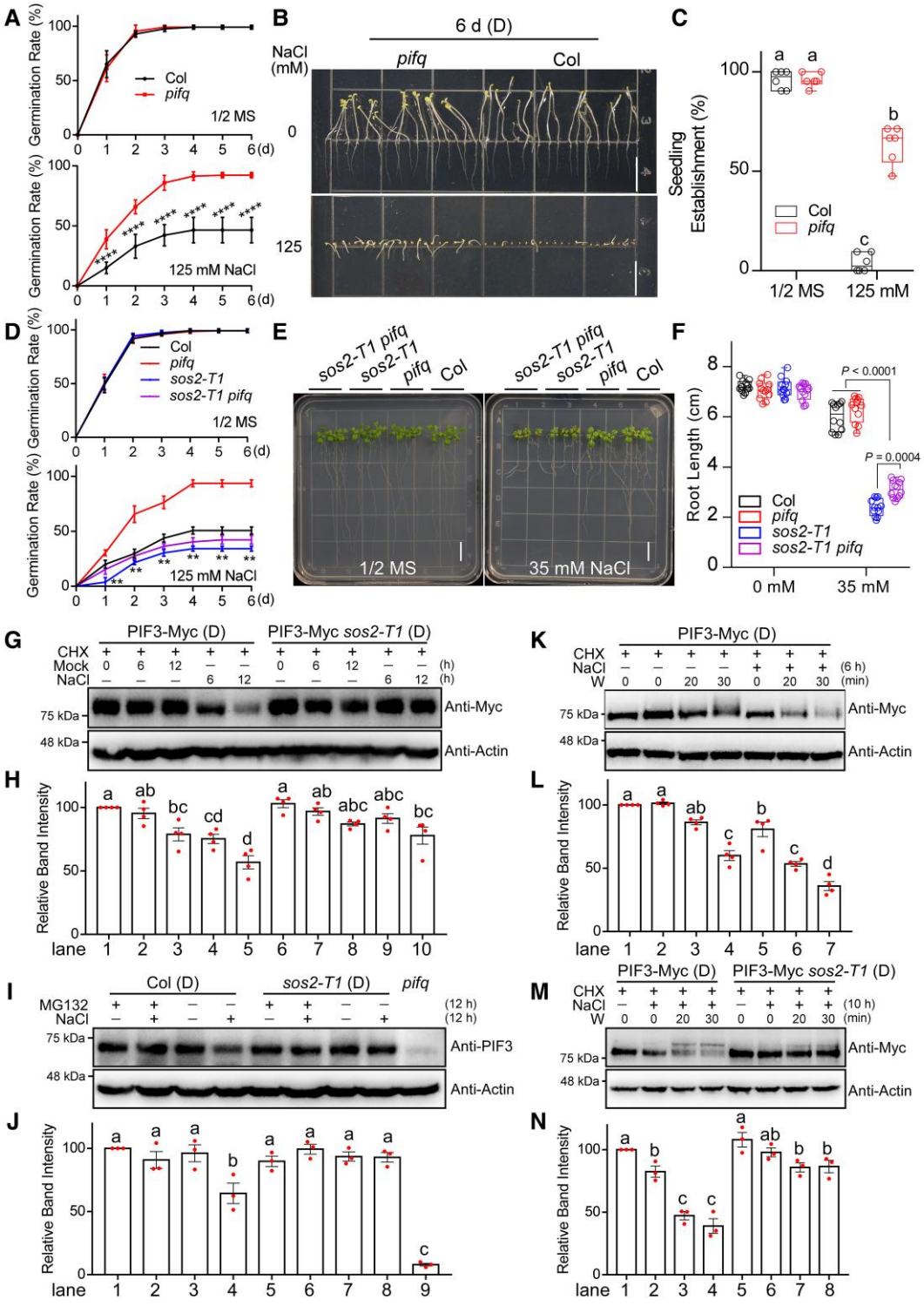

Figure 4. SOS2 relieves the repressive effect of PIF1 and PIF3 on plant salt tolerance by mediating their degradation in response to salt stress. **A)** Germination rate measurement. Imbibed seeds of WT (Col) and *pifq* mutants were sown on 1/2 MS medium containing 0 or 125 mM NaCl in darkness, and then seed germination rates were calculated at the indicated times. Germination was defined as the first sign of radicle tip emergence and scored daily until the 6th day of incubation. Data are the means ± SE ($n = 4$, each pool containing at least 45 seeds). ****$P < 0.0001$ (Student's *t*-test; **Supplemental Data Set 2**) for the indicated pairs of seeds. **B)** Growth of *pifq* seedlings is less sensitive to NaCl. WT (Col) and *pifq* seedlings were grown vertically on 1/2 MS medium containing 0 and 125 mM NaCl in the dark for 6 d. **C)** Seedling establishment rate measurements. Col and *pifq* seedlings were grown on 1/2 MS medium containing 0 or 125 mM NaCl in the dark conditions for 6 d. ($n = 6$), each pool containing 40 seedlings. Different letters represent significant differences determined by two-way ANOVA with Tukey's post hoc test ($P < 0.05$; **Supplemental Data Set 2**). **D)** Germination rate measurement. Imbibed seeds of Col, *sos2-T1*, *pifq*, and *sos2-T1 pifq* seeds were sown on 1/2 MS medium containing 0 or 125 mM

(continued)

that whereas the translated PIF1-Myc and PIF3-Myc proteins were relatively stable in the dark without salt stress, they were steadily degraded in response to NaCl treatments (Fig. 4, G and H, Supplemental Fig. S13A), indicating that salt stress decreases the stability of PIF1 and PIF3 proteins in the dark.

To determine the role of SOS2 in salt-induced destabilization of PIF1 and PIF3 proteins, we generated homozygous *Pro35S:PIF1-Myc* and *Pro35S:PIF3-Myc* seedlings in the *sos2-T1* mutant background and compared the degradation of translated PIF1-Myc and PIF3-Myc proteins in response to NaCl treatment. Intriguingly, our immunoblot data showed that salt-induced degradation of PIF1-Myc and PIF3-Myc was remarkably slower in *sos2-T1* than in Col background (Fig. 4, G and H, Supplemental Fig. S13A), indicating that SOS2 mediates salt-induced destabilization of PIF1 and PIF3 proteins. Moreover, the addition of MG132, an inhibitor of 26S proteasomes, could efficiently inhibit the degradation of PIF1-Myc and endogenous PIF3 proteins in salt-treated Col seedlings (Fig. 4, I and J, Supplemental Fig. S13B), indicating that PIF1 and PIF3 proteins are degraded via the 26S proteasome pathway in response to salt stress.

It has been well documented that phytochromes interact with PIFs and induce their rapid phosphorylation and degradation upon light exposure (Al-Sady et al. 2006; Oh et al. 2006; Nozue et al. 2007; Shen et al. 2007, 2008; Lorrain et al. 2008). To investigate whether dark-experienced salt stress could modulate light-induced degradation of PIF proteins, 4-d-old etiolated *Pro35S:PIF3-Myc* transgenic plants were treated with mock or 100 mM NaCl in the dark, and then subjected to light exposure. Interestingly, we observed that the PIF3-Myc proteins were degraded faster upon light exposure in the seedlings pre-treated with salt stress in the dark (Fig. 4, K and L). To further verify this conclusion, 4-d-old etiolated Col and 2 individual *Pro35S:Myc-SOS2*^{T168D} transgenic lines were treated with white light for 30 min and then subjected to immunoblot assays. We observed that whereas light irradiation induced the degradation of endogenous PIF3, the degradation was much faster in *Pro35S:Myc-SOS2*^{T168D} transgenic plants than in Col seedlings (Supplemental Fig. S14), indicating that the superactive SOS2 resulted in faster degradation of PIF3 proteins in the light.

To further investigate whether the salt-activated SOS2 could modulate light-induced degradation of PIF3, 4-d-old *Pro35S:PIF3-Myc* and *Pro35S:PIF3-Myc sos2-T1* transgenic plants were treated with mock or 100 mM NaCl in the dark, and then subjected to light exposure. Notably, the degradation of PIF3-Myc was much slower upon light exposure in the absence of SOS2 (Fig. 4, M and N). These data indicate that dark-experienced salt stress accelerates SOS2-mediated degradation of PIFs in response to light.

SOS2 physically interacts with PIFs

To investigate whether SOS2 directly interacts with the PIF proteins, we first performed pull-down assays using purified recombinant His-tagged SOS2, MBP tag, and MBP-tagged PIF1/PIF3/PIF4/PIF5 proteins. Our data showed that His-SOS2 was able to pull down MBP-PIF1, MBP-PIF3, MBP-PIF4, and MBP-PIF5, but not the MBP tag alone (Supplemental Fig. S15). In addition, GST-tagged SOS2, but not GST alone, was able to pull down His-PIF1 and PIF3 as well (Fig. 5, A and B). These data indicated that SOS2 interacts with PIF1, PIF3, PIF4, and PIF5 in vitro. Further in vitro pull-down assays showed that the N-terminal kinase domain but not the C-terminal regulatory domain of SOS2 (Guo et al.

Figure 4. (Continued)
NaCl in darkness, and then seed germination rates were calculated at the indicated times. Germination was defined as the first sign of radicle tip emergence and scored daily until the 6th day of incubation. Error bars represent SD ($n = 4$, each pool containing at least 45 seeds). $^{**}P < 0.01$ (Student's *t*-test; **Supplemental Data Set 2**) for the comparisons between *sos2-T1* and *sos2-T1 pifq* seeds. **E and F)** Phenotypes **(E)** and root lengths **(F)** of Col, *sos2-T1*, *pifq*, and *sos2-T1 pifq* seedlings grown on control (1/2 MS) or NaCl (35 mM) media in white light. The seedlings were first grown vertically on 1/2 MS medium without NaCl in continuous white light for 7 d, and then transferred to 1/2 MS medium containing 0 or 35 mM NaCl and grown under continuous white light for additional 5 d. In **(E)**, scale bar = 1 cm, in **(F)**, $n = 12$. Different letters represent significant differences determined by two-way ANOVA with Tukey's post hoc test ($P < 0.05$; **Supplemental Data Set 2**). **G and H)** Immunoblots show that SOS2 mediates the degradation of the translated PIF3-Myc proteins in response to NaCl treatments. *Super:PIF3-Myc* and *Super:PIF3-Myc sos2-T1* seedlings grown in darkness for 4 d were treated with CHX, together with or without 100 mM NaCl, for 6 or 12 h. Representative pictures are shown in **(G)** and the relative levels of PIF3-Myc proteins are shown in **(H)**. **I and J)** Immunoblots showing that MG132 could efficiently inhibit the degradation of endogenous PIF3 proteins in salt-treated Col seedlings. Col and *sos2-T1* mutants grown in darkness for 4 d were treated with MG132, together with or without 100 mM NaCl, for 12 h. Representative pictures are shown in **(I)** and the relative levels of PIF3 proteins are shown in **(J)**. **K and L)** Immunoblots showing that the PIF3-Myc proteins were degraded faster upon light exposure in the seedlings pre-treated with salt stress in the dark. *Super:PIF3-Myc* seedlings grown in darkness for 4 d were treated with CHX, together with or without 100 mM NaCl, and incubated in darkness for additional 6 h, and then transferred to white light for the indicated times. Representative pictures are shown in **(K)** and the relative levels of PIF3 proteins are shown in **(L)**. **M and N)** Immunoblots show that the degradation of PIF3-Myc was much slower upon light exposure in the absence of SOS2. *Super:PIF3-Myc pif3-3* and *Super:PIF3-Myc sos2-T1* grown in darkness for 4 d were treated with CHX and 100 mM NaCl, and incubated in darkness for additional 10 h, and then transferred to white light for the indicated times. Representative pictures are shown in **(M)** and the relative levels of PIF3 proteins are shown in **(N)**. In **(G)**, **(I)**, **(K)**, and **(M)**, anti-Actin was used as a sample loading control. Relative band intensities of endogenous PIF3 or PIF3-Myc proteins normalized to those of the loading controls, respectively. The error bars in **(H)**, **(J)**, **(L)**, and **(N)** represent SE from 3 or 4 independent assays, with each assay using a different pool of seedlings. Different letters represent significant differences by one-way ANOVA with Tukey's post hoc test ($P < 0.05$; **Supplemental Data Set 2**).

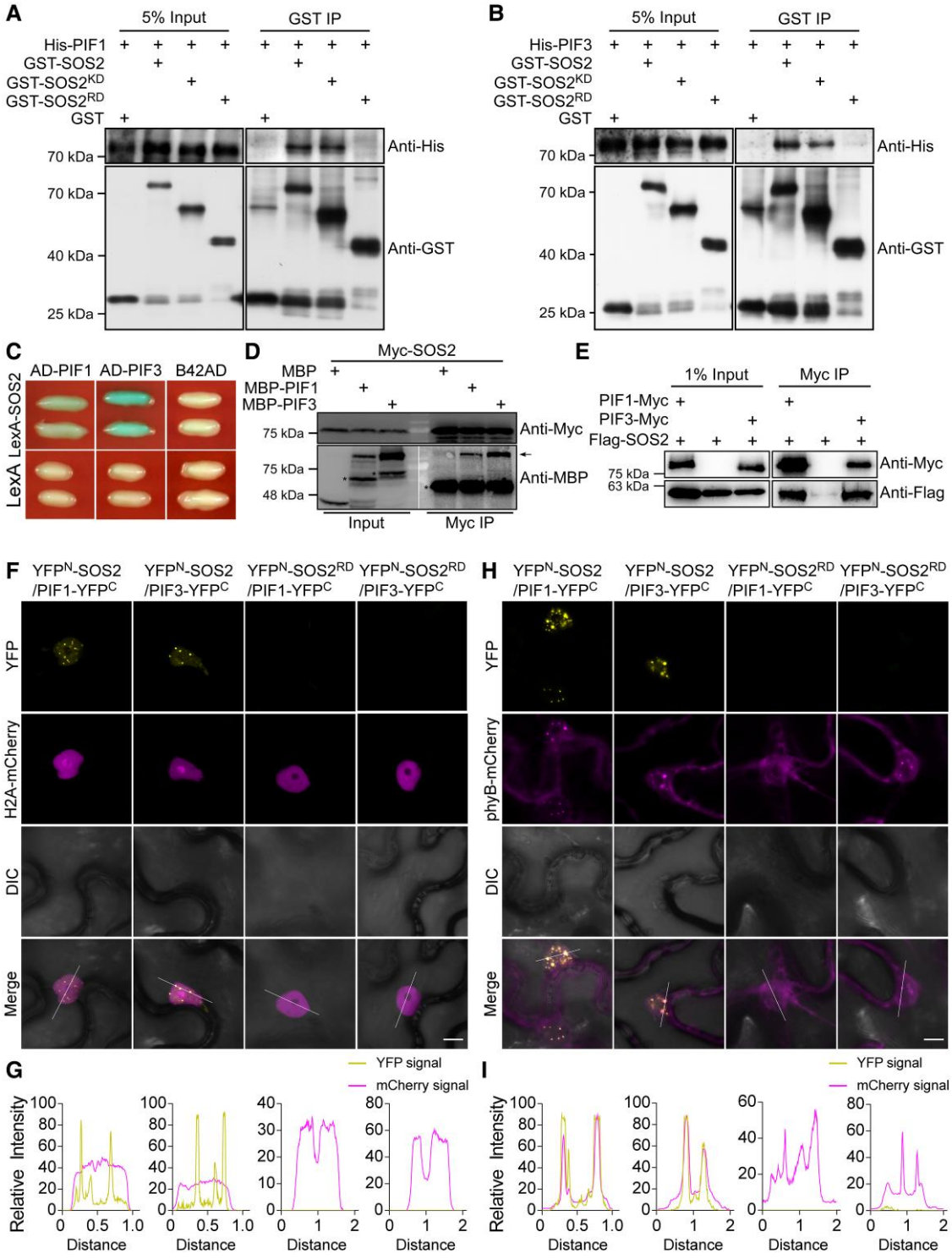

Figure 5. SOS2 physically interacts with PIF1 and PIF3. **A and B)** Pull-down assays showing that GST-tagged SOS2 and SOS2^{KD}, but not GST-tagged SOS2RD or GST alone, could pull down His-tagged PIF1 **(A)** and PIF3 **(B)** in vitro. **C)** Yeast two-hybrid assays show that both PIF1 and PIF3 interacted with SOS2 in yeast cells. **D)** Semi-in vivo pull-down assays showing that MBP-PIF1 and MBP-PIF3 proteins were coprecipitated with Myc-SOS2. Total proteins were extracted from 4-d-old *Pro35S:Myc-SOS2* seedlings grown in white light, and then equivalent amounts of protein extract (500 μg each sample) were incubated with 2 μg of MBP-PIF1, MBP-PIF3, or MBP for 2 h. Then, the mixtures were incubated with anti-Myc Affinity Gel (Sigma-Aldrich), and the total and precipitated proteins were subjected to immunoblot analyses with antibodies against Myc and MBP, respectively. The asterisks denote the nonspecific bands; the arrow denotes the corresponding protein bands of PIF proteins. **E)** Co-IP assays showing that SOS2 interacted with PIF1 and PIF3 in vivo. Flag-SOS2 and PIF1-Myc or PIF3-Myc fusion proteins were transiently expressed in Arabidopsis leaf protoplasts. The total proteins were extracted and incubated with anti-Myc Affinity Gel (Sigma-Aldrich). The total (1% input) and precipitated proteins were

(continued)

2001) is responsible for interacting with PIF1 and PIF3 (Fig. 5, A and B). Yeast two-hybrid assays further showed that SOS2 interacts with PIF1 and PIF3 in yeast (*Saccharomyces cerevisiae*) cells (Fig. 5C).

To further verify the interactions between SOS2 and PIF1/PIF3, we performed semi-in vivo co-IP assays using MBP-PIF1 and MBP-PIF3 proteins purified from *E. coli* and the total proteins extracted from *Pro35S:Myc-SOS2* seedlings grown in continuous white light. Our results showed that both MBP-PIF1 and MBP-PIF3 proteins, but not MBP alone, were coprecipitated with Myc-SOS2 proteins by the anti-Myc antibodies (Fig. 5D). In addition, we performed co-IP assays by transiently co-expressing PIF1/PIF3-Myc and Flag-SOS2 in Arabidopsis leaf protoplasts. As shown in Fig. 5E, Flag-SOS2 was coprecipitated by PIF1-Myc and PIF3-Myc (Fig. 5E).

To further verify the interactions between PIF1/PIF3 and SOS2 *in planta*, we performed BiFC assays by transiently co-expressing PIF1/PIF3-YFP^{C} (full-length PIF1/PIF3 fused with the C-terminal domain of YFP) and YFP^{N}-SOS2 in *N. benthamiana* leaves. As shown in Fig. 5, F and G and Supplemental Fig. S16A, whereas YFP fluorescence was not detectable when YFP^{N}-SOS2 co-transformed with GUS-YFP^{C}, or YFP^{N}-SOS2RD (regulatory domain of SOS2 fused with N-terminal domain of YFP) and YFP^{N}-GUS co-transformed with PIF1/PIF3-YFP^{C}, co-expression of YFP^{N}-SOS2 and PIF1-YFP^{C} or PIF3-YFP^{C} led to strong YFP fluorescence in the nucleus. Notably, we observed that the interactions between SOS2 and PIF1/PIF3 led to the formation of nuclear bodies (Fig. 5, F and G; Supplemental Fig. S16A). Collectively, our data demonstrate that SOS2 interacts with PIF1 and PIF3 in plant cells.

Since SOS2 interacts with both phyA/phyB and PIFs (Figs. 2, G to P and 5, A to G), and PIFs could interact with phyA/phyB (Ni et al. 1998; Huq and Quail 2002; Huq et al. 2004; Khanna et al. 2004), we next asked whether these 3 types of proteins co-localize in living plant cells. To this end, we transiently co-expressed YFP^{N}-SOS2 or YFP^{N}-SOS2RD and PIF1/PIF3-YFP^{C} together with phyA/phyB-mCherry in *N. benthamiana* leaves. Intriguingly, we observed that both phyA-mCherry and phyB-mCherry co-localized with the nuclear bodies formed by YFP^{N}-SOS2 and PIF1/PIF3-YFP^{C} (Fig. 5, H and I; Supplemental Fig. S16, B and C), indicating that SOS2 co-localize with both phyA/phyB and PIFs in living plant cells.

To further elucidate the associations of phyA/phyB, SOS2, and PIF1/PIF3 in vivo, we performed additional co-IP assays by transiently co-expressing *Myc-PIF1/PIF3*, *Flag-SOS2*, and *phyA/phyB-GFP* in Arabidopsis leaf protoplasts. As shown in Supplemental Fig. S16, D and E, both Flag-SOS2 and phyA/phyB-GFP were coprecipitated by anti-Myc antibodies in the presence of Myc-PIF1/PIF3, indicating PIF1/PIF3 associated with SOS2 and phyA/phyB in vivo. Taken together, our data demonstrated that SOS2 associates with the phy-PIF modules to positively regulate plant salt tolerance.

SOS2 directly phosphorylates PIFs and decreases the stability of PIF1/PIF3 in response to light

It was interesting to notice that less amounts of shifted PIF3-Myc proteins were produced in *sos2* mutants upon light exposure (Fig. 4M). These observations suggest that SOS2 may mediate the phosphorylation of PIF3-Myc proteins in vivo. To investigate whether SOS2 directly phosphorylates PIF proteins, we performed in vitro kinase assays using recombinant MBP-PIF1, MBP-PIF3, MBP-PIF4, MBP-PIF5, MBP-PIF7, and His-SOS2 proteins purified from *E. coli*. Our results showed that PIF1, PIF3, PIF4, and PIF5, but not PIF7 were phosphorylated in the presence of SOS2 (Fig. 6A; Supplemental Fig. S17), indicating that PIF1, PIF3, PIF4, and PIF5 are the substrates of SOS2 in vitro.

Further analyses revealed that SOS2 predominantly phosphorylates the N-terminal regions of both PIF1 and PIF3 (Fig. 6, B and C; Supplemental Fig. S18A). To further map the SOS2-mediated phosphorylation sites, we performed in vitro kinase assays coupled with LC-MS/MS analyses and identified 4 sites, respectively, in the N-terminal domains of PIF1 and PIF3 proteins (Supplemental Fig. S18, A and B). We mutated each of the 4 SOS2 phosphorylation sites of PIF3, respectively, or mutated them together to phosphorylation-deficient alanines, and our kinase assay data showed that, indeed, the PIF3 mutant proteins (PIF3^{4A} and PIF3^{4D}) were less phosphorylated by SOS2 in vitro (Fig. 6D; Supplemental Fig. S19). Together, our data demonstrate that SOS2 phosphorylates PIF1 and PIF3 proteins in vitro and in vivo.

To investigate the role of 4 SOS2 phosphorylation sites in regulating PIF3 protein stability and function in vivo, we generated transgenic lines expressing PIF3-Myc, PIF3^{4A}-Myc (4 sites mutated to phosphorylation-deficient alanines), or PIF3^{4D}-Myc (4 sites mutated to phosphorylation-mimic aspartic acids) in the *pif3-3* mutant background under the control of the constitutive Super promoter. Multiple independent homozygous transgenic lines were obtained for

Figure 5. (Continued)
examined by immunoblotting using anti-Myc and anti-Flag antibodies, respectively. **F)** BiFC assays showing the interactions between SOS2 and PIF1/PIF3 in *N. benthamiana* leaf cells. H2A-mCherry, the nuclear localization marker. The regulatory domain of SOS2 (SOS2RD) was used as the negative control. Scale bar = 20 μm. **G)** The fluorescence intensities (YFP and mCherry signals) over the white lines shown in **(F)** were scanned using the ImageJ plot profile tool. The *y*-axes indicate relative pixel intensity. Distance indicates the relative positions on the white lines. **H)** BiFC assays show that SOS2 co-localizes with both phyB and PIFs in the nucleus of *N. benthamiana* leaf cells. The regulatory domain of SOS2 (SOS2RD) was used as the negative control. Scale bar = 20 μm. **I)** The fluorescence intensities (YFP and mCherry signals) over the white lines shown in **(H)** were scanned using the ImageJ plot profile tool. The *y*-axes indicate relative pixel intensity. Distance indicates the relative positions on the white lines.

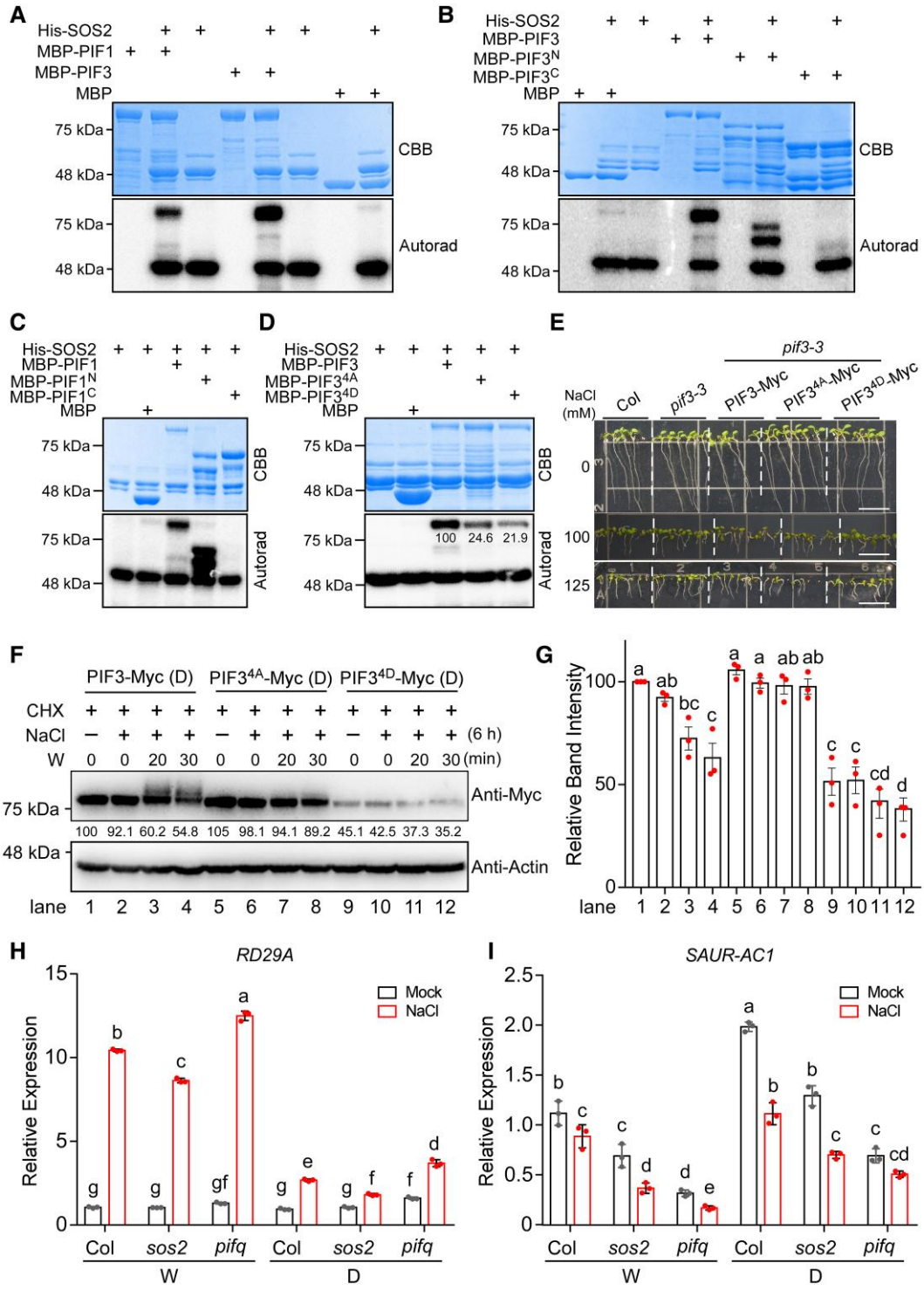

Figure 6. SOS2 directly phosphorylates PIF1 and PIF3 and decreases the stability of PIF3 in response to light. **A)** In vitro kinase assays show that SOS2 directly phosphorylates PIF1 and PIF3 proteins. The top panel shows CBB-stained SDS-PAGE gel containing His-SOS2, MBP-PIF1/PIF3, and MBP proteins, and the bottom panel shows autoradiograph indicating SOS2 autophosphorylation (bottom bands) and MBP-PIF1/PIF3 phosphorylation (top bands). **B and C)** In vitro kinase assays show that SOS2 predominantly phosphorylates the N-terminal domains of PIF3 **(B)** and PIF1 **(C)**. The top panel shows CBB-stained SDS-PAGE gel containing His-SOS2, MBP, full-length and truncated PIF1/PIF3 proteins, and the bottom panel shows autoradiograph indicating SOS2 autophosphorylation (bottom bands) and MBP-PIF1/PIF3 phosphorylation (top bands). **D)** In vitro kinase assays show that SOS2 phosphorylates 4 sites (Ser-151, Ser-152, Ser-153, and Ser-307) of PIF3. The top panel shows CBB-stained SDS-PAGE gel containing His-SOS2, MBP, WT, and mutated PIF3 proteins (PIF^{4A}: non-phosphorylatable variant; PIF^{4D}: phosphomimic variant), and the bottom panel shows autoradiograph indicating SOS2 autophosphorylation (bottom bands) and MBP-PIF1/PIF3 phosphorylation (top bands). **E)** Growth of Col, *pif3-3*, *Super:PIF3-Myc*, *Super:*$PIF3^{4A}$*-Myc pif3-3*, and *Super:*$PIF3^{4D}$*-Myc pif3-3* seedlings under the treatment of NaCl in the light. Seeds of indicated genotypes

(continued)

each transgene, and 1 representative line was selected for *Super:PIF3-Myc*, *Super:PIF3^{4A}-Myc*, and *Super:PIF3^{4D}-Myc*, respectively, based on the criteria that the expression levels of transgenic *PIF3-Myc* were largely comparable in these lines (Supplemental Fig. S20). We then compared the seedling growth of these lines on 1/2 MS medium containing 0, 100, or 125 mM NaCl in the light. Interestingly, we observed that whereas *Super:PIF3^{4D}-Myc* lines exhibited similar seedling growth as *pif3-3* seedlings under all tested concentrations of NaCl, *Super:PIF3^{4A}-Myc* lines displayed significantly retarded seedling growth particularly under the treatments of 100 and 125 mM NaCl in the light (Fig. 6E). These data indicate that mutation of 4 SOS2 phosphorylation sites of PIF3 to alanines caused *Super:PIF3^{4A}-Myc* transgenic seedlings hypersensitive to salt stress.

To gain molecular insight into reduced salt tolerance of *Super:PIF3^{4A}-Myc* transgenic seedlings, we first examined the levels of PIF3-Myc, PIF3^{4A}-Myc, and PIF3^{4D}-Myc proteins in the respective seedlings grown in the dark. Notably, we observed that the steady state level of PIF3^{4D}-Myc was much lower than those of PIF3-Myc and PIF3^{4A}-Myc proteins in the dark (Fig. 6, F and G), indicating that mutation of 4 SOS2 phosphorylation sites to aspartic acid led to decreased stability of mutant PIF3 proteins. In addition, after we treated 4-d-old etiolated *Super:PIF3-Myc*, *Super:PIF3^{4A}-Myc*, and *Super:PIF3^{4D}-Myc* seedlings with 100 mM NaCl for 6 h in the dark and then transferred them to light for different times, we observed that both PIF3-Myc and PIF3^{4D}-Myc proteins were degraded rapidly upon light exposure; by contrast, the degradation of PIF3^{4A}-Myc was much slower than that of PIF3-Myc and PIF3^{4D}-Myc proteins (Fig. 6, F and G). Collectively, our data demonstrate that SOS2 phosphorylation of PIF3 at these 4 sites decreases the stability of PIF3, thus relieving the repressive effect of PIF3 on plant salt tolerance.

Finally, we performed quantitative real-time PCR (qPCR) analyses to examine whether SOS2 could modulate the expression of *SMALL AUXIN UP RNA FROM ARABIDOPSIS COLUMBIA1* (*SAUR-AC1*), *INDOLE-3-ACETIC ACID INDUCIBLE 19* (*IAA19*), *RESPONSIVE TO DESICCATION 29A* (*RD29A*), and *COLD-REGULATED 15A* (*COR15A*), 4 PIF-regulated genes involved in either growth regulation or salt stress response (Zhang et al. 2013; Jiang et al. 2017; Li et al. 2020). Our data indicated that whereas the expression of *SAUR-AC1* was regulated by SOS2 in both light and dark conditions with or without salt stress, the expression of *IAA19*, *RD29A*, and *COR15A* was regulated by SOS2 only after salt stress (Fig. 6, H and I; Supplemental Fig. S21). Our data demonstrate that SOS2 modulates the expression of PIF-regulated genes involved in regulating growth or salt response.

Discussion

Light and soil salinity are major environmental factors that coordinately control plant growth and development. However, the mechanisms underlying the crosstalk between light and salt stress signaling pathways in plants remain poorly understood. In this study, we showed that SOS2, a key kinase of the SOS signaling pathway, regulates plant salt tolerance according to their light environment. Our data demonstrated that whereas PIFs accumulate in the dark and act as negative regulators of plant salt tolerance, SOS2 interacts with and directly phosphorylates PIF1 and PIF3, thus facilitating the rapid turnover of PIF1 and PIF3 and relieving their repressive effect on plant salt tolerance (Fig. 7). Notably, our data indicated that whereas SOS2 kinase activity is not significantly induced by salt stress in darkness, salt-induced SOS2 activity is drastically enhanced in the light by photoactivated phytochromes (Fig. 2, D and E; Fig. 7), demonstrating that salt and light signals synergistically promote SOS2 kinase activity.

Together, data in this study demonstrated that SOS2 acts as a hub in integrating external light signals and internal salt stress pathways, thus ensuring optimal fitness to stress conditions.

After germination occurs, buried seedlings first undergo skotomorphogenic development in the dark and then switch to photomorphogenic development when they emerge from soil into sunlight (Li et al. 2011; Cheng et al. 2021). PIFs act as pivotal transcription factors repressing photomorphogenesis (Leivar and Quail 2011) and must be promptly removed to allow photomorphogenesis to occur upon light irradiation. Consistently, it has been well established that phytochromes (predominantly phyA and phyB)

Figure 6. (Continued)
were sown on ½ MS medium containing 0, 100, or 125 mM NaCl, and then grown in the light for 7 d. Scale bar = 1 cm. **F and G)** Immunoblots and quantification showing that the degradation of PIF3^{4A}-Myc was much slower than that of PIF3-Myc and PIF3^{4D}-Myc proteins upon light exposure. *Super:PIF3-Myc*, *Super:PIF3^{4A}-Myc pif3-3*, and *Super:PIF3^{4D}-Myc pif3-3* seedlings grown in darkness for 4 d were treated with CHX and 100 mM NaCl, and incubated in darkness for additional 6 h, and then transferred to white light for the indicated times. Anti-Actin was used as a sample loading control. Numbers below the immunoblot indicate the relative band intensities of PIF3-Myc proteins normalized to those of the loading controls, respectively. The ratio of the first band was set to 100 for the blot. Representative pictures are shown in **(F)**, and the relative levels of Myc-tagged proteins are shown in **(G)**. Error bars in **(G)** represent SE from 3 independent assays. Different letters represent significant differences by one-way ANOVA with Tukey's post hoc test ($P < 0.05$; **Supplemental Data Set 2**). **H and I)** qPCR analyses showing the expression levels of *RD29A* **(H)** and *SAUR-AC1* **(I)** in Col, *sos2-T1*, and *pifq* seedlings grown in white light or dark conditions for 5 d and then treated with mock or 100 mM NaCl for 6 h. Error bars represent the SD of 3 technical replicates. Data are normalized to *tubulin3*. Different letters represent significant differences by two-way ANOVA with Tukey's post hoc test ($P < 0.05$; **Supplemental Data Set 2**).

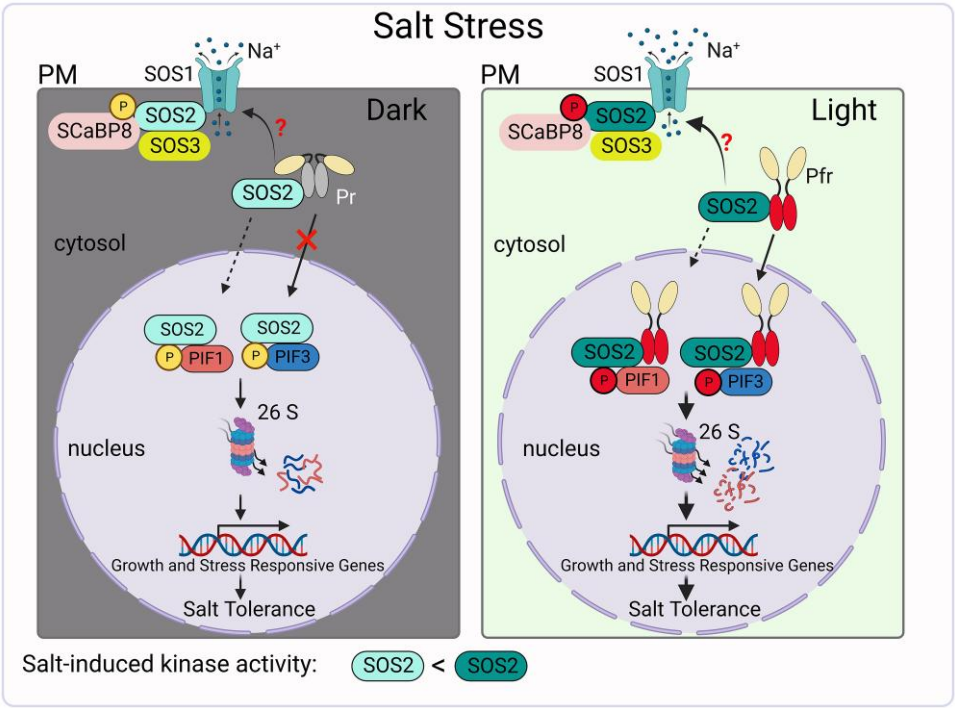

Figure 7. A working model showing that phytochromes promote plant salt tolerance by enhancing SOS2-mediated phosphorylation and degradation of PIF1 and PIF3 in the light. In the dark, SOS2 kinase activity is mildly induced by salt stress, and salt-activated SOS2 interacts with and phosphorylates PIF1 and PIF3, thus relieving their repressive effect on plant salt tolerance. In the light, photoactivated phytochromes (Pfr; mainly phyA and phyB) translocate into the nucleus, interact with SOS2, and enhance SOS2 kinase activity in response to salt stress. Highly activated SOS2 phosphorylates PIF1 and PIF3 and facilitates the more rapid turnover of PIF1 and PIF3 under salt stress in the light. On the other hand, photoactivated phytochromes may also promote SOS2 activity in the cytosol, thereby leading to enhanced SOS1 activity at the plasma membrane (PM).

mediate rapid phosphorylation and subsequent 26S proteasome-mediated degradation by directly interacting with PIFs in response to light (Al-Sady et al. 2006; Castillon et al. 2007). Based on these backgrounds, our data in this study provide a scenario where seedlings struggle to survive if they germinate in the saline soil: accumulation of PIFs allows seedlings to elongate their hypocotyls, but at the expense of decreased salt tolerance, in darkness under the cover of soil (Fig. 7). However, once the seedlings reach the sunlight, photoactivated phytochromes enhance the kinase activity of SOS2 and facilitate much rapid removal of PIFs and transition to photomorphogenic development. Thus, the seedlings are more tolerant to salt stress in the light, but grow slowly with much-reduced levels of PIFs (Fig. 7). In the absence of salt stress, however, SOS2 is not significantly activated irrespective of the light conditions, which can prevent unnecessary salt response and avoid unnecessary energy expense. Together, our results indicate that the SOS2-PIF module plays a central role in the trade-off between growth limitation and salt tolerance, and that the energy-efficient performance of the SOS2-PIF module is governed by phytochromes.

Although it was shown that SOS2 is a nucleocytoplasmic protein (Kim et al. 2007, 2013; Quan et al. 2007), the function of nuclear SOS2 in salt stress response remains completely obscure. Our data demonstrate the function of nuclear SOS2 in salt stress response based on the following lines of evidence. First, it was shown that PIFs are nuclear proteins (Ni et al. 1998; Huq and Quail 2002) and that phytochromes rapidly translocate into the nucleus in response to light (Fankhauser and Chen 2008; Klose et al. 2015), while our confocal microscopy results revealed that SOS2 co-localize with both phyA/phyB and PIFs in the nuclear bodies of plant cells (Fig. 5, H and I; Supplemental Fig. S16, B and C). Second, phytochromes promote plant salt tolerance by enhancing SOS2 kinase activity rather than its protein levels (Fig. 2, F and G; Supplemental Fig. S7). Third, our genetic analyses showed that nuclear-localized NLS-YFP-SOS2^{T168D}, but not the NLS-YFP-SOS2, could partially rescue the salt-sensitive phenotype of *phyA-211* mutants (Fig. 3, D to F; Supplemental Fig. S9). Fourth, our gene expression analyses showed that SOS2 modulates the expression of PIF target genes in response to salt stress (Fig. 6, H and I; Supplemental Fig. 21). Together, our data demonstrate that nuclear SOS2 presumably modulates the expression of salt stress-responsive genes by decreasing the stability of PIFs, thus playing a key role in regulating plant salt tolerance.

However, our data by no means suggest a minor role of cytosolic SOS2 in salt stress response. By contrast, SOS2-activated SOS1, a plasma membrane Na^+/H^+

antiporter, is essential for plant salt tolerance by extruding Na^+ from the cytosol to the apoplast (Shi et al. 2000; Qiu et al. 2002; Quintero et al. 2011). It seems likely that photoactivated phytochromes may also promote the activity of cytosolic SOS2 (Fig. 7), given that the interactions of SOS2 with phytochromes were observed in the cytosol as well (Fig. 2, M to P; Supplemental Fig. S6, D and E), and that phytochromes also trigger cytosolic events in response to light (Rosler et al. 2007; Li et al. 2011).

Interestingly, the transcript and protein levels of SOS1 were shown to be diurnally regulated (Park et al. 2016). Together with our findings that PIFs increase, whereas photoactivated phytochromes decrease the Na^+ accumulation in Arabidopsis seedlings grown under salt stress (Supplemental Figs. S4 and S12), it seems likely that phyA/phyB and PIFs might regulate plant salt tolerance in the light through modulating the accumulation or activity of SOS1. Two possible mechanisms may be involved in phytochrome-mediated regulation of SOS1 activity under salt stress: phytochromes may activate SOS1 through PIF-dependent transcriptional regulation of *SOS1* expression, or promote SOS2 activity in the cytosol, thereby leading to enhanced SOS1 activity at the plasma membrane. The exact regulatory mechanisms underlying phytochrome regulation of SOS1 activity need to be verified in future studies.

It is well established that SOS2 is specifically activated by the salt-induced $[Ca^{2+}]_{cyt}$ elevation (Quan et al. 2007; Ma et al. 2019). Interestingly, we showed that phytochromes enhance salt-activated SOS2 activity in the light (Fig. 2, F and G). Since light also stimulates an increase in intracellular calcium concentration (Wayne and Hepler 1985; Stoelzle et al. 2003), whether increased calcium concentration is involved in phytochrome-mediated enhancement of SOS2 activity remains to be investigated in future studies. Since phyA and phyB were not shown to regulate the levels of endogenous SOS2 proteins (Supplemental Fig. S7), it will be interesting to test several other possibilities in future research. For example, whether phytochromes may regulate SOS2 nucleocytoplasmic partitioning (e.g. facilitating translocation of SOS2 from the cytosol to the nucleus in the light) is an intriguing question. In addition, since it was shown that the phosphorylation of the SOS2 Thr-168 residue greatly promotes SOS2 kinase activity (Guo et al. 2001; Barajas-Lopez et al. 2018), it will be intriguing to investigate whether phytochromes enhance SOS2 kinase activity by facilitating the phosphorylation of the SOS2 Thr-168 residue.

A recent study showed that plants exhibit enhanced tolerance to cold stress in various light conditions than in darkness and that CRYPTOCHROME2 (CRY2)-mediated blue light signaling enhances freezing tolerance (Li et al. 2021). Together, it is evident that plants adjust their strategies to abiotic stress according to their light environment, and that photoreceptors-triggered signaling pathways enhance plant tolerance to abiotic stress.

To summarize, our study demonstrates that SOS2 plays an essential role in regulating plant salt tolerance and that this regulatory role of SOS2 is modulated by light. Our study thus provides molecular insights into the understanding of how plants obtain optimal fitness to stress conditions according to their light environment.

Materials and methods

Plant materials and growth conditions

The *A. thaliana* Columbia (Col) accession was used as the WT in this study unless otherwise indicated. The *sos2-T1* (SALK_016683) was obtained from the Arabidopsis Biological Resource Center (ABRC) (http://www.arabidopsis.org/abrc/). The *phyA-211* (Reed et al. 1994), *phyB-9* (Reed et al. 1993), *pif1-1* (Huq et al. 2004), *pif3-1* (Monte et al. 2004), *pif3-3* (Monte et al. 2004), *pif4-2* (Leivar et al. 2008a), *pif5-3* (Khanna et al. 2008), *pifq* (*pif1-1 pif3-3 pif4-2 pif5-3*; Leivar et al. 2008b), *Pro35S:PIF1-Myc* (Qi et al. 2020), *35S:PIF3-Myc* (Park et al. 2004), *Pro35S:PIF4* (de Lucas et al. 2008), *Pro35S:PIF5-HA* (Shen et al. 2007), *ProPHYA:phyA-NLS-GFP phyA-211* (Genoud et al. 2008), *Pro35S:phyB-GFP phyB-9* (Zheng et al. 2013), and *Pro35S:Myc-SOS2* (Lin et al. 2009) have been described previously. The *phyA-211 phyB-9*, *pifq sos2-T1*, and *phyA-211 sos2-T1* mutants were generated by genetic crossing.

To grow Arabidopsis seedlings, the seeds were first sterilized and then sown on 1/2 MS, pH 5.8, supplemented with 1% (w/v) sucrose and 0.3% or 0.6% (w/v) phytagel (Cat#P8169, Sigma-Aldrich). After 2-d stratification at 4 °C, the seeds in Petri dishes were pre-irradiated with white light (F17T8/TL841 bulb, Philips) for 12 h and then incubated at 22 °C in complete darkness (D) or continuous white (PAR, 100 μmol m^{-2} s^{-1}), blue (B; 5 μmol m^{-2} s^{-1}), FR (10 μmol m^{-2} s^{-1}), or R (20 μmol m^{-2} s^{-1}) light in growth chambers (Percival Scientific) for indicated times.

To grow *N. benthamiana*, the seeds were first sown on soil (nutrient soil:vermiculite; [1:1; v/v]) and then placed at the greenhouse (24 ± 1 °C with 14 h/10 h [light/dark]) cycle for about 7 to 10 d. Subsequently, the young seedlings were transplanted into culture boxes individually to grow for another 10 to 15 d in the greenhouse.

Plasmid construction and generation of transgenic plants

The AD-PIF1 and AD-PIF3 constructs were described previously (Qi et al. 2020). To generate the LexA-SOS2 construct, the full-length coding sequence of *SOS2* was cloned into the EcoR*I*-Sal*I* sites of the LexA vector (Clontech) using the primers shown in Supplemental Data Set 1.

The GST-SOS2, GST-$SOS2^{KD}$, GST-$SOS2^{RD}$, His-SOS2, His-PHYA, His-PHYB, His-PIF1, and His-PIF3 constructs were described previously (Guo et al. 2001; Dong et al. 2020; Yan et al. 2020). To generate the MBP-PIF1, MBP-$PIF1^N$ (1–219 aa), MBP-$PIF1^C$ (220–478 aa), MBP-PIF3, MBP-$PIF3^N$ (1–320 aa), and MBP-$PIF3^C$ (321–524 aa) constructs, the respective coding sequences were amplified by

PCR using the primers shown in Supplemental Data Set 1 and then cloned into the *SalI-EcoR*I sites of the pMAL-c5x vector (NEB), respectively. To generate MBP-PIF3^{4A} and MBP-PIF3^{4D} constructs, the Mut Express II Fast Mutagenesis Kit V2 (Vazyme) was used with the MBP-PIF3 plasmid as the template and the primers shown in Supplemental Data S1 according to the manufacturer's instructions.

The YFP^{N}-SOS2, YFP^{N}-GUS, and GUS-YFP^{C} constructs were described previously (Zhou et al. 2014, Li et al. 2020). To generate the YFP-SOS2RD, the coding sequence of SOS2RD (268-446 aa) was cloned into the BamH*I*-Kpn*I* sites of the pSPYNE vector (Waadt and Kudla 2008) using the primers shown in Supplemental Data Set 1. To generate PIF1-YFP^{C} and PIF3-YFP^{C} constructs, the respective coding sequences were amplified using the primers shown in Supplemental Data Set 1 and cloned into Sal*I*-Kpn*I* sites of the pSPYCE (MR) vector (Waadt and Kudla 2008). To generate phyA-YFP^{C} and phyB-YFP^{C} constructs, the respective coding sequences were amplified using the primers shown in Supplemental Data Set 1 and cloned into Spe*I*-Xho*I* sites of the pSPYCE (MR) vector (Waadt and Kudla 2008). To generate phyA^{C323A}-YFP^{C} construct, the Mut Express II Fast Mutagenesis Kit V2 (Vazyme) was used with the phyA-YFP^{C} plasmid as the template and the primers shown in Supplemental Data S1 according to the manufacturer's instructions.

The SOS2-nLUC, phyA-nLUC, cLUC-phyB, GUS-nLUC, and cLUC-GUS constructs were described previously (Yan et al. 2020, Dong et al. 2020, Li et al. 2020). To generate the cLUC-SOS2 construct, the full-length coding sequence of *SOS2* was cloned into the *Kpn*I-*Sal*I sites of the *Pro*35S:cLUC vector (Chen et al. 2008) using the primers shown in Supplemental Data Set 1.

To generate the *ProUBQ10:NLS-YFP-SOS2* construct, the coding sequences of the *NLS*, *YFP*, and *SOS2* were amplified, respectively, and then cloned into the pCAMBIA1390 vector using the ClonExpress Ultra One Step Cloning Kit (Vazyme, #C115-01). To generate the *Pro35S:Myc-SOS2*^{T168D} and *ProUBQ10:NLS-YFP-SOS2*^{T168D} construct, the *Pro35S:Myc-SOS2* and *ProUBQ10:NLS-YFP-SOS2* plasmid was used as the template, respectively, using the Mut Express II Fast Mutagenesis Kit V2 (Vazyme) and the primers shown in Supplemental Data Set 1 according to the manufacturer's instructions.

To generate the *Super:PIF1-Myc* and *Super:PIF3-Myc* constructs, the indicated coding sequences of WT *PIF1*/*PIF3* were fused with Myc, respectively, and then cloned into the *Sal*I-*Kpn*I sites of the pSuper1300 vector (Liu et al. 2017) using the primers shown in Supplemental Data Set 1. To generate *Super:PIF3*^{4A}*-Myc* and *Super:PIF3*^{4D}*-Myc* constructs, the Mut Express II Fast Mutagenesis Kit V2 (Vazyme) was used with the *Super:PIF3-Myc* plasmid as the template and the primers shown in Supplemental Data S1 according to the manufacturer's instructions.

The *Super:phyB-mCherry* construct was described previously (Yan et al. 2020). To generate the *Super:phyA-mCherry* construct, the indicated coding sequences of *phyA* were fused with mCherry and then cloned into the Kpn*I*-Spe*I* sites of the pSuper1300 vector (Liu et al. 2017).

To generate the *Super:PIF1-Myc*, *Super:PIF3-Myc*, *Super:PIF3*^{4A}*-Myc*, *Super:PIF3*^{4D}*-Myc*, *Pro35S:Myc-SOS2*, *Pro35S:Myc-SOS2* ^{T168D}, *ProUBQ10:NLS-YFP-SOS2*, and *ProUBQ10:NLS-YFP-SOS2*^{T168D} transgenic plants, the corresponding constructs were transformed into *Agrobacterium tumefaciens* (strain GV3101), and then transformed into Col, *sos2-T1*, *pif3-3*, *phyA-211*, or *phyA-211 phyB-9* mutants, respectively, by the floral dip method (Clough and Bent 1998).

All of the primers used in plasmid construction are listed in Supplemental Data Set 1, and all of the constructs were confirmed by sequencing prior to usage in various assays. The transgenic plants were selected on the MS medium supplemented with hygromycin B (30 mg L^{-1}) or glufosinate (10 mg L^{-1}), and the T3 homozygous transgenic lines were used for further research.

BiFC assays

The BiFC assays were performed as described previously (Waadt and Kudla 2008; Horstman et al. 2014). Briefly, the indicated pairs of constructs were transfected into *N. benthamiana* leaves for transient expression by *A. tumefaciens* (GV3101)-mediated infiltration. After infiltration, plants were allowed to grow for another 2 or 3 d, and the YFP signals were detected and captured by a confocal laser scanning microscope (lasers: 488 nm, 15%; 561 nm, 15%; gains: 600; pinhole: 100 μm) (ZEISS LSM 880). The relative signal intensity was measured by ImageJ.

Total protein extraction and immunoblotting

For immunoblots detecting PIF1-Myc and PIF3-Myc proteins, total proteins were extracted as described previously (Qiu et al. 2017). Briefly, the Arabidopsis seedlings (50 mg) were treated with mock (1/2 MS) or NaCl (100 mM) along with or without 100 μM MG132 (Sigma) and/or 200 μM CHX (Sigma), then harvested and ground in 150 μL extraction buffer (100 mM Tris-HCl, pH 7.5, 100 mM NaCl, 5 mM EDTA, pH 8.0, 5% [w/v] SDS, 20% [v/v] glycerol, 20 mM DTT, 40 mM β-mercaptoethanol, 2 mM PMSF, 1× EDTA-free complete protease inhibitor cocktail [Roche], 80 μM MG132 [Sigma], 80 μM MG115 [Sigma], 1% phosphatase inhibitor cocktail [Sigma], 10 mM *N*-ethylmaleimide). The samples were immediately boiled for 10 min, and then centrifuged at 16,000 × *g* for 10 min at room temperature. Proteins in the supernatant were used in the subsequent immunoblot assays.

Primary antibodies used in this study include anti-GST (1:1,000 [v/v], Cat#G7781; Sigma-Aldrich), anti-His (1:1,000 [v/v], Cat#1029; Sigma-Aldrich), anti-MBP (1:3,000 [v/v], Cat#E8032S; NEW ENGLAND BioLabs, NEB), anti-Flag (1:3,000 [v/v], Cat#F3165; Sigma-Aldrich), anti-GFP (1:3,000 [v/v], Cat#11814460001; Roche), anti-phyA (1:1,000 [v/v]; Zhang et al. 2018), anti-phyB (1:1,000 [v/v]; Dong et al. 2020), anti-PIF3 (1:1,000 [v/v], Cat#AS163954; Agrisera), anti-HSP (1:1,000 [v/v], Cat#AbM51099-31-PU; Beijing

Protein Innovation), anti-Myc (1:3,000 [v/v], Cat#01219; CWBIO), and anti-Actin (1:3,000 [v/v], Cat#01265; CWBIO). The anti-SOS2 antibodies (1:500 [v/v]) were made by Beijing Protein Innovation and are described in the companion study by Han et al. (2023). Secondary antibodies used in this study include goat anti-rabbit IgG (H+L), HRP (1:3,000 [v/v], Cat#80781121; Bioeasytech), goat anti-mouse IgG (H+L), HRP (1:3,000 [v/v], Cat#80781124; Bioeasytech), and rabbit anti-goat IgG (H+L), HRP (1:3,000 [v/v], Cat#133371; ZSGB-BIO).

Immunoblotting assays were performed as described previously (Ma et al. 2019). Briefly, total samples containing the protein of interest were resolved by gel electrophoresis and then transferred to a PVDF membrane. The nonspecific binding sites on the PVDF membrane were blocked by 5% (w/v) milk. Subsequently, primary antibodies bind to the protein antigen and then are targeted by the labeled secondary antibodies. Finally, the chemiluminescence signals are detected by a cold charge-coupled device (CCD) (FUSION SOLO 4M, VILBER).

In vitro pull-down, semi-in vivo, and in vivo co-IP assays

For in vitro pull-down assays, 10 μg of recombinant bait proteins (GST-SOS2, GST-SOS2-KD, GST-SOS2-RD, GST, or His-SOS2) and 10 μg of prey proteins (His-PIF1, His-PIF3, His-PHYA, His-PHYB, MBP-PIF1, MBP-PIF3, or MBP) were added into 1 mL binding buffer containing 50 mM Tris-HCl, pH 7.5, 100 mM NaCl, 0.6% (v/v) Triton X-100, and 0.2% (v/v) glycerol. After incubation for 2 h at 4 °C, the mixtures were incubated with prewashed Glutathione Sepharose 4B beads (GE Healthcare) or Ni-NTA Agarose (MCLAB, Cat#NINTA-300) for another 2 h at 4 °C. After 5 times of washing with the binding buffer, the pulled-down proteins were eluted in 2× SDS loading buffer at 100 °C for 10 min, and detected by immunoblotting with anti-GST, anti-His, or anti-MBP antibodies, respectively.

For semi-in vivo co-IP assays, 4-d-old etiolated *Pro35S:Myc-SOS2* seedlings were harvested, ground into powder in liquid nitrogen, and then homogenized in the precooled protein extraction buffer containing 10 mM Tris-HCl, pH 7.6, 0.5% Nonidet-P40, 2 mM EDTA, 150 mM NaCl, 1× EDTA-free protease inhibitor cocktail (Roche). After centrifugation at 16,000 × *g* for 10 min, binding reactions were started by mixing equivalent amounts of total proteins (500 μg) with 2 μg of recombinant proteins (MBP-PIF1, MBP-PIF3, or MBP), respectively, in 1 mL of protein extraction buffer. The mixtures were incubated with prewashed anti-Myc Affinity Gel (Sigma-Aldrich) for 2 h at 4 °C. The beads were then washed 5 times with protein extraction buffer at 4 °C and eluted in 2× SDS loading buffer. The eluted proteins were detected by immunoblotting using anti-Myc and anti-MBP antibodies, respectively.

For in vivo co-IP assays in Arabidopsis leaf protoplasts, purified bait (*Pro35S:Myc-SOS2*, *Super:PIF1-Myc* and *Super:PIF3-Myc*) and prey (*Super:phyA-GFP*, *Super:phyB-GFP*, and *Pro35S:Flag-SOS2*) plasmid pairs were transiently expressed in Arabidopsis leaf protoplasts. After overnight incubation, the protoplasts were lysed by protein extraction buffer (10 mM Tri-HCl, pH 7.6, 0.5% Nonidet-P40, 2 mM EDTA, 150 mM NaCl, 1× EDTA-free protease inhibitor cocktail, Roche), centrifuged, and the left supernatant was incubated with prewashed anti-Myc Affinity Gel (Sigma-Aldrich) at 4 °C for 2 h. After 5-time washes, the co-immunoprecipitated proteins were detected by immunoblotting using anti-Myc, anti-Flag, and anti-GFP antibodies, respectively.

Yeast two-hybrid assays

The two-hybrid assays were performed as described previously (Qi et al. 2020). Briefly, the indicated combinations of LexA-SOS2 and AD-PIF1, AD-PIF3, or empty vector were co-transformed into the yeast (*S. cerevisiae*) strain EGY48, respectively. The yeast transformants were selected on the SD/-Trp-Ura-His agar plates and then grown on the SD/Gal/Raf/-Trp-Ura-His agar plates containing X-Gal (5-bromo-4-chloro-3-indolyl-β-D-galactopyranoside) for blue color development. Photos were taken after incubation at 30 °C for 18–24 h.

Na^+ content measurement

Seeds were germinated vertically on 1/2 MS medium under continuous white light for 6 d. Seedlings were transferred to 1/2 MS or 1/2 MS with NaCl as indicated. A pool containing more than 60 individual plants represented 1 biological replicate. Shoots and roots were harvested separately and oven-dried at 80 °C for at least 48 h. After weighing, samples were digested into 68% (w/v) HNO_3, and then a dilution series was created using 1% hydrochloric acid. The Na^+ contents were determined using a 4100 MP-AES device (Agilent, Santa Clara, CA, USA).

qPCR analyses

Total RNA was extracted from 4-d-old seedlings with TRizol reagent (Invitrogen), followed by the reverse transcription using M-MLV reverse transcriptase (Promega). qPCR assays were performed with SYBR Premix Ex Taq kit (Takara), and specific gene primers were listed in Supplemental Data Set 1. qPCR was performed in triplicate for each sample, and the relative expression levels were normalized to that of *TUBULIN3* gene.

Protein purification and kinase assays

All His-, GST-, and MBP-fusion protein constructs were transformed into *E. coli* BL21 (DE3) cells, and the expression of recombinant proteins was induced by 0.5 mM isopropyl-β-D-thiogalactopyranoside for 12 h at 16 °C. Cells were collected, lysed, sonicated, and centrifuged, and then the His-tagged, MBP-tagged, or GST-tagged recombinant proteins in the supernatant were purified by Ni-NTA Agarose (MCLAB, Cat#NINTA-300), Amylose Resin (NEB, Cat#E8021S), or Glutathione Sepharose 4B beads (GE

Healthcare), respectively, according to the manufacturer's instructions.

For semi-in vivo kinase assays, *Pro35S:Myc-SOS2* or *Pro35S:Myc-SOS2 phyA phyB* seedlings grown under different light conditions were treated with mock or 100 mM NaCl for 12 h and then harvested. The seedlings were ground to powder in liquid nitrogen and then homogenized in 1 mL precooled IP buffer (10 mM Tris-HCl, pH 7.6, 0.5% Nonidet-P40, 2 mM EDTA, 150 mM NaCl, 1× EDTA-free protease inhibitor cocktail [Roche]). The proteins were centrifuged at 16,000 × *g* for 10 min at 4 °C and incubated with anti-Myc Affinity Gel (Sigma-Aldrich) for 2 h at 4 °C. Same amounts of immunoprecipitated Myc-SOS2 were used for the kinase assays using the His-SCaBP8 proteins as the substrates.

In vitro kinase assays were conducted as described previously (Lin et al. 2009). Briefly, the kinase and substrate proteins were mixed in 15 μL of kinase reaction buffer (20 mM Tris-HCl [pH 8.0], 5 mM $MgCl_2$, 1 mM $CaCl_2$, 10 mM ATP, and 1 mM DTT). Kinase assays were performed by adding 0.1 μL [γ-^{32}P] (1 μCi), and the mixtures were incubated at 30 °C for another 30 min. Reactions were stopped by adding 3 μL 6× SDS loading buffer and then boiling at 100 °C for 8 min. The resulting proteins were separated by 12% (w/v) SDS-PAGE gels and stained by Coomassie Brilliant Blue R 250, and then the gels were exposed to a phosphor screen (Amersham Biosciences). The isotopic signals were detected by a Typhoon 9410 phosphor imager (Amersham Biosciences) and quantified by the ImageQuant 5.0 software.

Mass spectrometry analysis

To identify the SOS2 phosphorylation sites in PIF1 and PIF3, 30 μg recombinant His-SOS2 were incubated together with 50 μg MBP-PIF1 or MBP-PIF3 proteins in the kinase reaction buffer (20 mM Tris-HCl [pH 8.0], 5 mM $MgCl_2$, 1 mM $CaCl_2$, 10 mM ATP, and 1 mM DTT) at 30 °C for 30 min. The protein mixtures were desalted using the ultrafiltration spin columns (30 kDa, 500 μL, Sartorius, Gottingen, Germany), washed with 50 mM NH_4HCO_3, then reduced with 50 mM DTT at 56 °C, and then alkylated with 200 mM iodoacetamide in the dark. Then, the proteins were digested with trypsin (1:50) at 37 °C overnight. The digested peptides were diluted with 0.1% FA and subjected to nano LC-MS analysis using the nano-Acquity nano HPLC (Waters, Milford, MA, USA) coupled with a Thermo Q-Exactive high-resolution mass spectrometer (Thermo Scientific, Waltham, MA, USA).

LCI assays

The indicated pairs of constructs were infiltrated into *N. benthamiana* leaves as described previously (Chen et al. 2008). After infiltration, the *N. benthamiana* plants were grown under a 16-h-light/8-h-dark cycle for another 2 or 3 d. Before imaging, the blade back of the infiltrated leaves was sprayed with 1 mM luciferin (the substrate of luciferase) and incubated in darkness for 5 min. The LUC signals were collected with the cold CCD camera (Nikon-L936; Andor Tech) at −110 °C within 10 or 15 exposures. Relative LUC intensities were analyzed by using the WinView32 software.

Microscopy

To detect the subcellular localization of SOS2, homozygous *ProUBQ10:NLS-YFP-SOS2* and *ProUBQ10:NLS-YFP-SOS2^{T168D}* seedlings in *phyA-211* or *sos2* mutant background were grown in continuous white light for 4 d, and then the YFP signals were captured by using the confocal laser scanning microscope (Lasers: 488 nm, 15%; 561 nm, 15%; gains: 600; pinhole: 100 μm) (ZEISS LSM 880).

Phenotypic analyses

The germination assays were performed as described previously (Qi et al. 2020; Nie et al. 2022). Briefly, the indicated seeds (at least 45 seeds for each genotype at each time point) harvested at the same time were sown on 1/2 MS medium containing various concentrations of NaCl. Germination was defined as the first sign of radicle tip emergence, and the germination rates were determined as a percentage of germinated seeds against the total seeds plated.

For the root growth and fresh weight assays, the indicated seeds were sown on 1/2 MS medium without NaCl, grown vertically under continuous white light for 7 d, and then the seedlings with similar sizes and at similar developmental stages were transferred to MS medium containing indicated concentrations of NaCl, and allowed to grow for additional 5–8 d. Primary root lengths or fresh weights were measured as described previously (Lin et al. 2009). The rates of seedling establishment were based on the criteria defined by previous studies (Yadukrishnan et al. 2020; Peng et al. 2022) that hypocotyls and cotyledons should emerge completely in established seedlings.

Quantification and statistical analyses

Protein quantification was performed with ImageJ. One-way ANOVA, two-way ANOVA, or Student's *t*-test were performed with GraphPad Prism 7.00. Different letters represent significant differences at $P < 0.05$. Values are represented as means ± standard deviation or means ± standard error of the mean. See Supplemental Data Set 2 for the results of all statistical analyses.

Accession numbers

Sequence data from this article can be found in the Arabidopsis Genome Initiative or GenBank/EMBL databases under the following accession numbers: *SOS2* (AT5G35410), *SCaBP8* (AT4G33000), *PIF1* (AT2G20180), *PIF3* (AT1G09530), *PIF4* (AT2G43010), *PIF5* (AT3G59060), *PHYA* (AT1G09570), *PHYB* (AT2G18790), *RD29A* (AT5G52310), *SAUR-AC1* (AT4G38850), *IAA19* (AT3G15540), *COR15A* (AT2G42540), *TUBULIN3* (AT5G62700), *EF1α* (AT1G07940).

Acknowledgments

We thank Drs Peter Quail and Chuanyou Li for the PIF-related seeds, and Dr Christian Fankhauser for the *ProPHYA:phyA-NLS-GFP phyA-211* seeds.

Author contributions

Y.G., L.M., Jig.L., and R.H. designed research. L.M., R.H., H.L., X.L., X.Z., Jia.L., H.F., Y.H., L.S., Y.Y., and H.Z. performed research. Y.G., Jig.L., Y-Q.Y., and F.T. discussed and interpreted the data. Y.G., Jig.L., L.M., and R.H. wrote the paper.

Supplemental data

The following materials are available in the online version of this article.

Supplemental Figure S1. PhyA and phyB positively regulate plant salt tolerance in the light.

Supplemental Figure S2. PhyA positively regulates plant salt tolerance in the light.

Supplemental Figure S3. Phenotypic analysis of soil-grown *phyA* mutant in response to salt stress.

Supplemental Figure S4. *phyA* Mutant seedlings accumulate Na^+ in response to salt stress.

Supplemental Figure S5. Genotyping of the *sos2-T1* mutant.

Supplemental Figure S6. PhyB physically interacts with SOS2.

Supplemental Figure S7. The levels of SOS2 proteins are not significantly regulated by phyA and phyB.

Supplemental Figure S8. Nuclear-localized SOS2 functions in salt stress tolerance.

Supplemental Figure S9. NLS-YFP-SOS2 could not rescue the salt-sensitive phenotype of *phyA-211* mutants.

Supplemental Figure S10. PIFs negatively regulate plant salt tolerance.

Supplemental Figure S11. Mutation of 4 PIF genes partially rescues the salt-sensitive phenotype of *sos2* mutants.

Supplemental Figure S12. Mutation of 4 PIF genes partially reduces the highly accumulated Na^+ contents in *sos2* mutants.

Supplemental Figure S13. SOS2 mediates PIF1 degradation in response to salt stress.

Supplemental Figure S14. The superactive SOS2 promotes light-induced degradation of PIF3.

Supplemental Figure S15. SOS2 directly interacts with PIF1, PIF3, PIF4, and PIF5 in vitro.

Supplemental Figure S16. SOS2, PIF1/PIF3, and phyA/phyB proteins form a complex in vivo.

Supplemental Figure S17. SOS2 directly phosphorylates PIF4 and PIF5 in vitro.

Supplemental Figure S18. Mapping of SOS2 phosphorylation sites in PIF1 and PIF3 proteins.

Supplemental Figure S19. Verification of SOS2 phosphorylation sites in PIF3 in vitro.

Supplemental Figure S20. The transcript levels of PIF3-Myc in different transgenic seedlings.

Supplemental Figure S21. SOS2 modulates the expression of PIF-regulated genes involved in regulating growth or salt response.

Supplemental Data Set 1. Primers used in this study.

Supplemental Data Set 2. Summary of statistical analyses.

Funding

This work was supported by grants from the National Key R&D Program of China (2022YFA1303400 to Y.G.), the National Natural Science Foundation of China (31921001 to Y.G.; 32000216 to L.M.), and the China Postdoctoral Science Foundation (2019M660865 and 2020T130703 to L.M.).

Conflict of interest statement. The authors declare no conflict of interests.

References

Al-Sady B, Ni W, Kircher S, Schafer E, Quail PH. Photoactivated phytochrome induces rapid PIF3 phosphorylation prior to proteasome-mediated degradation. Mol Cell. 2006:**23**(3):439–446. https://doi.org/10.1016/j.molcel.2006.06.011

Albrecht V, Ritz O, Linder S, Harter K, Kudla J. The NAF domain defines a novel protein-protein interaction module conserved in Ca^{2+}-regulated kinases. EMBO J. 2001:**20**(5):1051–1063. https://doi.org/10.1093/emboj/20.5.1051

Bae G, Choi G. Decoding of light signals by plant phytochromes and their interacting proteins. Annu Rev Plant Biol. 2008:**59**(1):281–311. https://doi.org/10.1146/annurev.arplant.59.032607.092859

Barajas-Lopez JD, Moreno JR, Gamez-Arjona FM, Pardo JM, Punkkinen M, Zhu JK, Quintero FJ, Fujii H. Upstream kinases of plant SnRKs are involved in salt stress tolerance. Plant J. 2018:**93**(1):107–118. https://doi.org/10.1111/tpj.13761

Bauer D, Viczian A, Kircher S, Nobis T, Nitschke R, Kunkel T, Panigrahi KC, Adam E, Fejes E, Schafer E, et al. Constitutive photomorphogenesis 1 and multiple photoreceptors control degradation of phytochrome interacting factor 3, a transcription factor required for light signaling in Arabidopsis. Plant Cell. 2004:**16**(6):1433–1445. https://doi.org/10.1105/tpc.021568

Bernardo-Garcia S, de Lucas M, Martinez C, Espinosa-Ruiz A, Daviere JM, Prat S. BR-dependent phosphorylation modulates PIF4 transcriptional activity and shapes diurnal hypocotyl growth. Genes Dev. 2014:**28**(15):1681–1694. https://doi.org/10.1101/gad.243675.114

Bu Q, Zhu L, Dennis MD, Yu L, Lu SX, Person MD, Tobin EM, Browning KS, Huq E. Phosphorylation by CK2 enhances the rapid light-induced degradation of phytochrome interacting factor 1 in Arabidopsis. J Biol Chem. 2011:**286**(14):12066–12074. https://doi.org/10.1074/jbc.M110.186882

Castillon A, Shen H, Huq E. Phytochrome interacting factors: central players in phytochrome-mediated light signaling networks. Trends Plant Sci. 2007:**12**(11):514–521. https://doi.org/10.1016/j.tplants.2007.10.001

Chen H, Zou Y, Shang Y, Lin H, Wang Y, Cai R, Tang X, Zhou JM. Firefly luciferase complementation imaging assay for protein-protein interactions in plants. Plant Physiol. 2008:**146**(2):323–324. https://doi.org/10.1104/pp.107.111740

Cheng MC, Kathare PK, Paik I, Huq E. Phytochrome signaling networks. Annu Rev Plant Biol. 2021:**72**(1):217–244. https://doi.org/10.1146/annurev-arplant-080620-024221

Cheng NH, Pittman JK, Zhu JK, Hirschi KD. The protein kinase SOS2 activates the Arabidopsis H^+/Ca^{2+} antiporter CAX1 to integrate calcium transport and salt tolerance. J Biol Chem. 2004:**279**(4):2922–2926. https://doi.org/10.1074/jbc.M309084200

Clough SJ, Bent AF. Floral dip: a simplified method for *Agrobacterium*-mediated transformation of *Arabidopsis thaliana*. Plant J. 1998:**16**(6):735–743. https://doi.org/10.1046/j.1365-313x.1998.00343.x

de Lucas M, Daviere JM, Rodriguez-Falcon M, Pontin M, Iglesias-Pedraz JM, Lorrain S, Fankhauser C, Blazquez MA, Titarenko E, Prat S. A molecular framework for light and gibberellin control of cell elongation. Nature. 2008:**451**(7177):480–484. https://doi.org/10.1038/nature06520

Dong X, Yan Y, Jiang B, Shi Y, Jia Y, Cheng J, Shi Y, Kang J, Li H, Zhang D, et al. The cold response regulator CBF1 promotes Arabidopsis hypocotyl growth at ambient temperatures. EMBO J. 2020:**39**(13):e103630. https://doi.org/10.15252/embj.2019103630

Fankhauser C, Chen M. Transposing phytochrome into the nucleus. Trends Plant Sci. 2008:**13**(11):596–601. https://doi.org/10.1016/j.tplants.2008.08.007

Feng XJ, Li JR, Qi SL, Lin QF, Jin JB, Hua XJ. Light affects salt stress-induced transcriptional memory of *P5CS1* in Arabidopsis. Proc Natl Acad Sci USA. 2016:**113**(51):E8335–E8343. https://doi.org/10.1073/pnas.1610670114

Genoud T, Schweizer F, Tscheuschler A, Debrieux D, Casal JJ, Schafer E, Hiltbrunner A, Fankhauser C. FHY1 Mediates nuclear import of the light-activated phytochrome A photoreceptor. PLoS Genet. 2008:**4**(8):e1000143. https://doi.org/10.1371/journal.pgen.1000143

Guo Y, Halfter U, Ishitani M, Zhu JK. Molecular characterization of functional domains in the protein kinase SOS2 that is required for plant salt tolerance. Plant Cell. 2001:**13**(6):1383–1400. https://doi.org/10.1105/TPC.010021

Halfter U, Ishitani M, Zhu JK. The Arabidopsis SOS2 protein kinase physically interacts with and is activated by the calcium-binding protein SOS3. Proc Natl Acad Sci USA. 2000:**97**(7):3735–3740. https://doi.org/10.1073/pnas.97.7.3735

Han R, Ma L, Lv Y, Qi L, Peng J, Li H, Zhou Y, Song P, Duan J, Li J, et al. SALT OVERLY SENSITIVE2 stabilizes phytochrome-interacting factors PIF4 and PIF5 to promote *Arabidopsis* shade avoidance. Plant Cell. 2023;**35**(8):2972–2996. https://doi.org/10.1093/plcell/koad119

Han X, Yu H, Yuan R, Yang Y, An F, Qin G. Arabidopsis transcription factor TCP5 controls plant thermomorphogenesis by positively regulating PIF4 activity. iScience. 2019:**15**:611–622. https://doi.org/10.1016/j.isci.2019.04.005

Hayes S, Pantazopoulou CK, van Gelderen K, Reinen E, Tween AL, Sharma A, de Vries M, Prat S, Schuurink RC, Testerink C, et al. Soil salinity limits plant shade avoidance. Curr Biol. 2019:**29**(10):1669–1676.e4. https://doi.org/10.1016/j.cub.2019.03.042

Horstman A, Tonaco IA, Boutilier K, Immink RG. A cautionary note on the use of split-YFP/BiFC in plant protein-protein interaction studies. Int J Mol Sci. 2014:**15**(6):9628–9643. https://doi.org/10.3390/ijms15069628

Huq E, Al-Sady B, Hudson M, Kim C, Apel K, Quail PH. Phytochrome-interacting factor 1 is a critical bHLH regulator of chlorophyll biosynthesis. Science. 2004:**305**(5692):1937–1941. https://doi.org/10.1126/science.1099728

Huq E, Quail PH. PIF4, A phytochrome-interacting bHLH factor, functions as a negative regulator of phytochrome B signaling in Arabidopsis. EMBO J. 2002:**21**(10):2441–2450. https://doi.org/10.1093/emboj/21.10.2441

Jiang B, Shi Y, Zhang X, Xin X, Qi L, Guo H, Li J, Yang S. PIF3 Is a negative regulator of the *CBF* pathway and freezing tolerance in Arabidopsis. Proc Natl Acad Sci USA. 2017:**114**(32):E6695–E6702. https://doi.org/10.1073/pnas.1706226114

Khanna R, Huq E, Kikis EA, Al-Sady B, Lanzatella C, Quail PH. A novel molecular recognition motif necessary for targeting photoactivated phytochrome signaling to specific basic helix-loop-helix transcription factors. Plant Cell. 2004:**16**(11):3033–3044. https://doi.org/10.1105/tpc.104.025643

Khanna R, Shen Y, Marion CM, Tsuchisaka A, Theologis A, Schafer E, Quail PH. The basic helix-loop-helix transcription factor PIF5 acts on ethylene biosynthesis and phytochrome signaling by distinct mechanisms. Plant Cell. 2008:**19**(12):3915–3929. https://doi.org/10.1105/tpc.107.051508

Kiegle E, Moore CA, Haseloff J, Tester MA, Knight MR. Cell-type-specific calcium responses to drought, salt and cold in the Arabidopsis root. Plant J. 2000:**23**(2):267–278. https://doi.org/10.1046/j.1365-313x.2000.00786.x

Kim WY, Ali Z, Park HJ, Park SJ, Cha JY, Perez-Hormaeche J, Quintero FJ, Shin G, Kim MR, Qiang Z, et al. Release of SOS2 kinase from sequestration with GIGANTEA determines salt tolerance in Arabidopsis. Nat Commun. 2013:**4**(1):1352. https://doi.org/10.1038/ncomms2357

Kim BG, Waadt R, Cheong YH, Pandey GK, Dominguez-Solis JR, Schültke S, Lee SC, Kudla J, Luan S. The calcium sensor CBL10 mediates salt tolerance by regulating ion homeostasis in Arabidopsis. Plant J. 2007:**52**(3):473–484. https://doi.org/10.1111/j.1365-313X.2007.03249.x

Klose C, Viczian A, Kircher S, Schafer E, Nagy F. Molecular mechanisms for mediating light-dependent nucleo/cytoplasmic partitioning of phytochrome photoreceptors. New Phytol. 2015:**206**(3):965–971. https://doi.org/10.1111/nph.13207

Knight H, Trewavas AJ, Knight MR. Calcium signalling in *Arabidopsis thaliana* responding to drought and salinity. Plant J. 1997:**12**(5):1067–1078. https://doi.org/10.1046/j.1365-313X.1997.12051067.x

Lee N, Choi G. Phytochrome-interacting factor from Arabidopsis to liverwort. Curr Opin Plant Biol. 2017:**35**:54–60. https://doi.org/10.1016/j.pbi.2016.11.004

Lee S, Paik I, Huq E. SPAs promote thermomorphogenesis by regulating the phyB-PIF4 module in Arabidopsis. Development. 2020:**147**(19):189233. https://doi.org/10.1242/dev.189233

Legris M, Ince YC, Fankhauser C. Molecular mechanisms underlying phytochrome-controlled morphogenesis in plants. Nat Commun. 2019:**10**(1):5219. https://doi.org/10.1038/s41467-019-13045-0

Leivar P, Monte E. PIFs: systems integrators in plant development. Plant Cell. 2014:**26**(1):56–78. https://doi.org/10.1105/tpc.113.120857

Leivar P, Monte E, Al-Sady B, Carle C, Storer A, Alonso JM, Ecker JR, Quail PH. The Arabidopsis phytochrome-interacting factor PIF7, together with PIF3 and PIF4, regulates responses to prolonged red light by modulating phyB levels. Plant Cell. 2008a:**20**(2):337–352. https://doi.org/10.1105/tpc.107.052142

Leivar P, Monte E, Oka Y, Liu T, Carle C, Castillon A, Huq E, Quail PH. Multiple phytochrome-interacting bHLH transcription factors repress premature seedling photomorphogenesis in darkness. Curr Biol. 2008b:**18**(23):1815–1823. https://doi.org/10.1016/j.cub.2008.10.058

Leivar P, Quail PH. PIFs: pivotal components in a cellular signaling hub. Trends Plant Sci. 2011:**16**(1):19–28. https://doi.org/10.1016/j.tplants.2010.08.003

Li J, Hiltbrunner A. Is the Pr form of phytochrome biologically active in the nucleus? Mol Plant. 2021:**14**(4):535–537. https://doi.org/10.1016/j.molp.2021.03.002

Li J, Li G, Wang H, Deng X. Phytochrome signaling mechanisms. Arabidopsis book. Vol. 9; 2011. p. e0148. https://doi.org/10.1199/tab.0148

Li Y, Shi Y, Li M, Fu D, Wu S, Li J, Gong Z, Liu H, Yang S. The CRY2-COP1-HY5-BBX7/8 module regulates blue light-dependent cold acclimation in Arabidopsis. Plant Cell. 2021:**33**(11):3555–3573. https://doi.org/10.1093/plcell/koab215

Li J, Zhou H, Zhang Y, Li Z, Yang Y, Guo Y. The GSK3-like kinase BIN2 is a molecular switch between the salt stress response and growth recovery in *Arabidopsis thaliana*. Dev Cell. 2020:**55**(3):367–380.6. https://doi.org/10.1016/j.devcel.2020.08.005

Lin H, Yang Y, Quan R, Mendoza I, Wu Y, Du W, Zhao S, Schumaker KS, Pardo JM, Guo Y. Phosphorylation of SOS3-LIKE CALCIUM BINDING PROTEIN8 by SOS2 protein kinase stabilizes their protein complex and regulates salt tolerance in Arabidopsis. Plant Cell. 2009:**21**(5):1607–1619. https://doi.org/10.1105/tpc.109.066217

Ling JJ, Li J, Zhu D, Deng XW. Noncanonical role of Arabidopsis COP1/SPA complex in repressing BIN2-mediated PIF3 phosphorylation and degradation in darkness. Proc Natl Acad Sci USA. 2017:**114**(13):3539–3544. https://doi.org/10.1073/pnas.1700850114

Liu J, Ishitani M, Halfter U, Kim CS, Zhu JK. The *Arabidopsis thaliana SOS2* gene encodes a protein kinase that is required for salt tolerance. Proc Natl Acad Sci USA. 2000:**97**(7):3730–3734. https://doi.org/10.1073/pnas.97.7.3730

Liu Z, Jia Y, Ding Y, Shi Y, Li Z, Guo Y, Gong Z, Yang S. Plasma membrane CRPK1-mediated phosphorylation of 14-3-3 proteins induces their nuclear import to fine-tune CBF signaling during cold response. Mol Cell. 2017:**66**(1):117–128.e5. https://doi.org/10.1016/j.molcel.2017.02.016

Lorrain S, Allen T, Duek PD, Whitelam GC, Fankhauser C. Phytochrome-mediated inhibition of shade avoidance involves degradation of growth-promoting bHLH transcription factors. Plant J. 2008:**53**(2):312–323. https://doi.org/10.1111/j.1365-313X.2007.03341.x

Ma L, Liu X, Lv W, Yang Y. Molecular mechanisms of plant responses to salt stress. Front Plant Sci. 2022:**13**:934877. https://doi.org/10.3389/fpls.2022.934877

Ma L, Ye J, Yang Y, Lin H, Yue L, Luo J, Long Y, Fu H, Liu X, Zhang Y, et al. The SOS2-SCaBP8 complex generates and fine-tunes an AtANN4-dependent calcium signature under salt stress. Dev Cell. 2019:**48**(5):697–709.e5. https://doi.org/10.1016/j.devcel.2019.02.010

Mizoguchi T, Wright L, Fujiwara S, Cremer F, Lee K, Onouchi H, Mouradov A, Fowler S, Kamada H, Putterill J, et al. Distinct roles of *GIGANTEA* in promoting flowering and regulating circadian rhythms in Arabidopsis. Plant Cell. 2005:**17**(8):2255–2270. https://doi.org/10.1105/tpc.105.033464

Mo W, Tang W, Du Y, Jing Y, Bu Q, Lin R. PHYTOCHROME-INTERACTING FACTOR-LIKE14 and SLENDER RICE1 interaction controls seedling growth under salt stress. Plant Physiol. 2020:**184**(1):506–517. https://doi.org/10.1104/pp.20.00024

Monte E, Tepperman JM, Al-Sady B, Kaczorowski KA, Alonso JM, Ecker JR, Li X, Zhang Y, Quail PH. The phytochrome-interacting transcription factor, PIF3, acts early, selectively, and positively in light-induced chloroplast development. Proc Natl Acad Sci USA. 2004:**101**(46):16091–16098. https://doi.org/10.1073/pnas.0407107101

Ni M, Tepperman JM, Quail PH. PIF3, A phytochrome-interacting factor necessary for normal photoinduced signal transduction, is a novel basic helix-loop-helix protein. Cell. 1998:**95**(5):657–667. https://doi.org/10.1016/S0092-8674(00)81636-0

Ni W, Xu SL, Chalkley RJ, Pham TN, Guan S, Maltby DA, Burlingame AL, Wang ZY, Quail PH. Multisite light-induced phosphorylation of the transcription factor PIF3 is necessary for both its rapid degradation and concomitant negative feedback modulation of photoreceptor phyB levels in Arabidopsis. Plant Cell. 2013:**25**(7):2679–2698. https://doi.org/10.1105/tpc.113.112342

Ni W, Xu SL, Gonzalez-Grandio E, Chalkley RJ, Huhmer AFR, Burlingame AL, Wang ZY, Quail PH. PPKs mediate direct signal transfer from phytochrome photoreceptors to transcription factor PIF3. Nat Commun. 2017:**8**(1):15236. https://doi.org/10.1038/ncomms15236

Nie K, Zhao H, Wang X, Niu Y, Zhou H, Zheng Y. The MIEL1-ABI5/MYB30 regulatory module fine tunes abscisic acid signaling during seed germination. J Integr Plant Biol. 2022:**64**(4):930–941. https://doi.org/10.1111/jipb.13234

Nozue K, Covington MF, Duek PD, Lorrain S, Fankhauser C, Harmer SL, Maloof JN. Rhythmic growth explained by coincidence between internal and external cues. Nature. 2007:**448**(7151):358–361. https://doi.org/10.1038/nature05946

Oh J, Park E, Song K, Bae G, Choi G. PHYTOCHROME INTERACTING FACTOR8 inhibits phytochrome A-mediated far-red light responses in Arabidopsis. Plant Cell. 2020:**32**(1):186–205. https://doi.org/10.1105/tpc.19.00515

Oh E, Yamaguchi S, Kamiya Y, Bae G, Chung WI, Choi G. Light activates the degradation of PIL5 protein to promote seed germination through gibberellin in Arabidopsis. Plant J. 2006:**47**(1):124–139. https://doi.org/10.1111/j.1365-313X.2006.02773.x

Ohta M, Guo Y, Halfter U, Zhu JK. A novel domain in the protein kinase SOS2 mediates interaction with the protein phosphatase 2C ABI2. Proc Natl Acad Sci USA. 2003:**100**(20):11771–11776. https://doi.org/10.1073/pnas.2034853100

Paik I, Chen F, Ngoc Pham V, Zhu L, Kim JI, Huq E. A phyB-PIF1-SPA1 kinase regulatory complex promotes photomorphogenesis in Arabidopsis. Nat Commun. 2019:**10**(1):4216. https://doi.org/10.1038/s41467-019-12110-y

Paik I, Kathare PK, Kim JI, Huq E. Expanding roles of PIFs in signal integration from multiple processes. Mol Plant. 2017:**10**(8):1035–1046. https://doi.org/10.1016/j.molp.2017.07.002

Pan Z, Zhao Y, Zheng Y, Liu J, Jiang X, Guo Y. A high-throughput method for screening Arabidopsis mutants with disordered abiotic stress-induced calcium signal. J Genet Genomics. 2012:**39**(5):225–235. https://doi.org/10.1016/j.jgg.2012.04.002

Park E, Kim J, Lee Y, Shin J, Oh E, Chung WI, Liu JR, Choi G. Degradation of phytochrome interacting factor 3 in phytochrome-mediated light signaling. Plant Cell Physiol. 2004:**45**(8):968–975. https://doi.org/10.1093/pcp/pch125

Park HJ, Qiang Z, Kim WY, Yun DJ. Diurnal and circadian regulation of salt tolerance in Arabidopsis. J Plant Biol. 2016:**59**(6):569–578. https://doi.org/10.1007/s12374-016-0317-8

Peng J, Wang M, Wang X, Qi L, Guo C, Li H, Li C, Yan Y, Zhou Y, Terzaghi W, et al. COP1 Positively regulates ABA signaling during Arabidopsis seedling growth in darkness by mediating ABA-induced ABI5 accumulation. Plant Cell. 2022:**34**(6):2286–2308. https://doi.org/10.1093/plcell/koac073

Pham VN, Kathare PK, Huq E. Phytochromes and phytochrome interacting factors. Plant Physiol. 2018:**176**(2):1025–1038. https://doi.org/10.1104/pp.17.01384

Qi L, Liu S, Li C, Fu J, Jing Y, Cheng J, Li H, Zhang D, Wang X, Dong X, et al. PHYTOCHROME-INTERACTING FACTORS interact with the ABA receptors PYL8 and PYL9 to orchestrate ABA signaling in darkness. Mol Plant. 2020:**13**(3):414–430. https://doi.org/10.1016/j.molp.2020.02.001

Qiu QS, Guo Y, Dietrich MA, Schumaker KS, Zhu JK. Regulation of SOS1, a plasma membrane Na^+/H^+ exchanger in *Arabidopsis thaliana*, by SOS2 and SOS3. Proc Natl Acad Sci USA. 2002:**99**(12):8436–8441. https://doi.org/10.1073/pnas.122224699

Qiu Y, Pasoreck EK, Reddy AK, Nagatani A, Ma W, Chory J, Chen M. Mechanism of early light signaling by the carboxy-terminal output module of Arabidopsis phytochrome B. Nat Commun. 2017:**8**(1):1905. https://doi.org/10.1038/s41467-017-02062-6

Quan R, Lin H, Mendoza I, Zhang Y, Cao W, Yang Y, Shang M, Chen S, Pardo JM, Guo Y. SCABP8/CBL10, A putative calcium sensor, interacts with the protein kinase SOS2 to protect Arabidopsis shoots from salt stress. Plant Cell. 2007:**19**(4):1415–1431. https://doi.org/10.1105/tpc.106.042291

Quintero FJ, Martinez-Atienza J, Villalta I, Jiang X, Kim WY, Ali Z, Fujii H, Mendoza I, Yun DJ, Zhu JK, et al. Activation of the plasma membrane Na^+/H^+ antiporter Salt-Overly-Sensitive 1 (SOS1) by phosphorylation of an auto-inhibitory C-terminal domain. Proc

Natl Acad Sci USA. 2011:**108**(6):2611–2616. https://doi.org/10.1073/pnas.1018921108

Quintero FJ, Ohta M, Shi H, Zhu JK, Pardo JM. Reconstitution in yeast of the Arabidopsis SOS signaling pathway for Na^+ homeostasis. Proc Natl Acad Sci USA. 2002:**99**(13):9061–9066. https://doi.org/10.1073/pnas.132092099

Rausenberger J, Tscheuschler A, Nordmeier W, Wust F, Timmer J, Schafer E, Fleck C, Hiltbrunner A. Photoconversion and nuclear trafficking cycles determine phytochrome A's Response profile to far-red light. Cell. 2011:**146**(5):813–825. https://doi.org/10.1016/j.cell.2011.07.023

Reed JW, Nagatani A, Elich TD, Fagan M, Chory J. Phytochrome A and phytochrome B have overlapping but distinct functions in Arabidopsis development. Plant Physiol. 1994:**104**(4):1139–1149. https://doi.org/10.1104/pp.104.4.1139

Reed JW, Nagpal P, Poole DS, Furuya M, Chory J. Mutations in the gene for the red/far-red light receptor phytochrome B alter cell elongation and physiological responses throughout Arabidopsis development. Plant Cell. 1993:**5**(2):147–157. https://doi.org/10.1105/tpc.5.2.147

Rosler J, Klein I, Zeidler M. Arabidopsis *fhl*/*fhy1* double mutant reveals a distinct cytoplasmic action of phytochrome A. Proc Natl Acad Sci USA. 2007:**104**(25):10737–10742. https://doi.org/10.1073/pnas.0703855104

Sakuraba Y, Bulbul S, Piao W, Choi G, Paek NC. Arabidopsis EARLY FLOWERING3 increases salt tolerance by suppressing salt stress response pathways. Plant J. 2017:**92**(6):1106–1120. https://doi.org/10.1111/tpj.13747

Sawa M, Nusinow DA, Kay SA, Imaizumi T. FKF1 And GIGANTEA complex formation is required for day-length measurement in Arabidopsis. Science. 2007:**318**(5848):261–265. https://doi.org/10.1126/science.1146994

Shen Y, Khanna R, Carle CM, Quail PH. Phytochrome induces rapid PIF5 phosphorylation and degradation in response to red-light activation. Plant Physiol. 2007:**145**(3):1043–1051. https://doi.org/10.1104/pp.107.105601

Shen H, Moon J, Huq E. PIF1 Is regulated by light-mediated degradation through the ubiquitin-26S proteasome pathway to optimize photomorphogenesis of seedlings in Arabidopsis. Plant J. 2005:**44**(6):1023–1035. https://doi.org/10.1111/j.1365-313X.2005.02606.x

Shen H, Zhu L, Castillon A, Majee M, Downie B, Huq E. Light-induced phosphorylation and degradation of the negative regulator PHYTOCHROME-INTERACTING FACTOR1 from Arabidopsis depend upon its direct physical interactions with photoactivated phytochromes. Plant Cell. 2008:**20**(6):1586–1602. https://doi.org/10.1105/tpc.108.060020

Shi H, Ishitani M, Kim C, Zhu JK. The *Arabidopsis thaliana* salt tolerance gene *SOS1* encodes a putative Na^+/H^+ antiporter. Proc Natl Acad Sci USA. 2000:**97**(12):6896–6901. https://doi.org/10.1073/pnas.120170197

Shi H, Quintero FJ, Pardo JM, Zhu JK. The putative plasma membrane Na^+/H^+ antiporter SOS1 controls long-distance Na^+ transport in plants. Plant Cell. 2002:**14**(2):465–477. https://doi.org/10.1105/tpc.010371

Shin AY, Han YJ, Baek A, Ahn T, Kim SY, Nguyen TS, Son M, Lee KW, Shen Y, Song PS, et al. Evidence that phytochrome functions as a protein kinase in plant light signalling. Nat Commun. 2016:**7**(1):11545. https://doi.org/10.1038/ncomms11545

Stoelzle S, Kagawa T, Wada M, Hedrich R, Dietrich P. Blue light activates calcium-permeable channels in Arabidopsis mesophyll cells via the phototropin signaling pathway. Proc Natl Acad Sci USA. 2003:**100**(3):1456–1461. https://doi.org/10.1073/pnas.0333408100

Tan T, Cai J, Zhan E, Yang Y, Zhao J, Guo Y, Zhou H. Stability and localization of 14-3-3 proteins are involved in salt tolerance in Arabidopsis. Plant Mol Biol. 2016:**92**(3):391–400. https://doi.org/10.1007/s11103-016-0520-5

van Zelm E, Zhang Y, Testerink C. Salt tolerance mechanisms of plants. Annu Rev Plant Biol. 2020:**71**(1):403–433. https://doi.org/10.1146/annurev-arplant-050718-100005

Waadt R, Kudla J. In planta visualization of protein interactions using bimolecular fluorescence complementation (BiFC). CSH Protoc. 2008;**2008**:pdb.prot4995. https://doi.org/10.1101/pdb.prot4995

Wayne R, Hepler PK. Red light stimulates an increase in intracellular calcium in the spores of *Onoclea sensibilis*. Plant Physiol. 1985:**77**(1):8–11. https://doi.org/10.1104/pp.77.1.8

Xin X, Chen W, Wang B, Zhu F, Li Y, Yang H, Li J, Ren D. Arabidopsis MKK10-MPK6 mediates red-light-regulated opening of seedling cotyledons through phosphorylation of PIF3. J Exp Bot. 2018:**69**(3):423–439. https://doi.org/10.1093/jxb/erx418

Yadukrishnan P, Rahul PV, Ravindran N, Bursch K, Johansson H, Datta S. CONSTITUTIVELY PHOTOMORPHOGENIC1 promotes ABA-mediated inhibition of post-germination seedling establishment. Plant J. 2020:**103**(2):481–496. https://doi.org/10.1111/tpj.14844

Yan Y, Li C, Dong X, Li H, Zhang D, Zhou Y, Jiang B, Peng J, Qin X, Cheng J, et al. MYB30 is a key negative regulator of Arabidopsis photomorphogenic development that promotes PIF4 and PIF5 protein accumulation in the light. Plant Cell. 2020:**32**(7):2196–2215. https://doi.org/10.1105/tpc.19.00645

Yang Y, Guo Y. Elucidating the molecular mechanisms mediating plant salt-stress responses. New Phytol. 2018a:**217**(2):523–539. https://doi.org/10.1111/nph.14920

Yang Y, Guo Y. Unraveling salt stress signaling in plants. J Integr Plant Biol. 2018b:**60**(9):796–804. https://doi.org/10.1111/jipb.12689

Yang Z, Wang C, Xue Y, Liu X, Chen S, Song C, Yang Y, Guo Y. Calcium-activated 14-3-3 proteins as a molecular switch in salt stress tolerance. Nature Commun. 2019:**10**(1):1199. https://doi.org/10.1038/s41467-019-09181-2

Zhang S, Li C, Zhou Y, Wang X, Li H, Feng Z, Chen H, Qin G, Jin D, Terzaghi W, et al. TANDEM ZINC-FINGER/PLUS3 is a key component of phytochrome A signaling. Plant Cell. 2018:**30**(4):835–852. https://doi.org/10.1105/tpc.17.00677

Zhang Y, Mayba O, Pfeiffer A, Shi H, Tepperman JM, Speed TP, Quail PH. A quartet of PIF bHLH factors provides a transcriptionally centered signaling hub that regulates seedling morphogenesis through differential expression-patterning of shared target genes in Arabidopsis. PLoS Genet. 2013:**9**(1):e1003244. https://doi.org/10.1371/journal.pgen.1003244

Zhao C, Zhang H, Song C, Zhu J-K, Shabala S. Mechanisms of plant responses and adaptation to soil salinity. Innovation. 2020;**1**(1):100017. https://doi.org/10.1016/j.xinn.2020.100017

Zheng X, Wu S, Zhai H, Zhou P, Song M, Su L, Xi Y, Li Z, Cai Y, Meng F, et al. Arabidopsis phytochrome B promotes SPA1 nuclear accumulation to repress photomorphogenesis under far-red light. Plant Cell. 2013:**25**(1):115–133. https://doi.org/10.1105/tpc.112.107086

Zhou H, Lin H, Chen S, Becker K, Yang Y, Zhao J, Kudla J, Schumaker KS, Guo Y. Inhibition of the Arabidopsis salt overly sensitive pathway by 14-3-3 proteins. Plant Cell. 2014:**26**(3):1166–1182. https://doi.org/10.1105/tpc.113.117069

Zhou Y, Xun Q, Zhang D, Lv M, Ou Y, Li J. TCP Transcription factors associate with PHYTOCHROME INTERACTING FACTOR 4 and CRYPTOCHROME 1 to regulate thermomorphogenesis in *Arabidopsis thaliana*. iScience. 2019:**15**:600–610. https://doi.org/10.1016/j.isci.2019.04.002

Zhu JK. Abiotic stress signaling and responses in plants. Cell. 2016:**167**(2):313–324. https://doi.org/10.1016/j.cell.2016.08.029

Zhu JK, Liu J, Xiong L. Genetic analysis of salt tolerance in Arabidopsis. Evidence for a critical role of potassium nutrition. Plant Cell. 1998:**10**(7):1181–1191. https://doi.org/10.1105/tpc.10.7.1181